THE UNIVERSITY OF MICHIGAN

COLLEGE OF ENGINEERING

DEPARTMENT OF ELECTRICAL AND COMPUTER ENGINEERING

Radiation Laboratory

FREE SPACE EC-135 SCALE MODEL MEASUREMENTS

by

V. V. Liepa and D. L. Dusette

Task Report No. 1, Contract F29601-76-C-0004
(5 August 1975 - 31 January 1976)

Prepared for:

Air Force Weapons Laboratory
Kirtland Air Force Base
New Mexico

14182-1-T = RL-2266

Ann Arbor, Michigan

1. INTRODUCTION

This is the first of the series of Task Reports on Contract F2 9601-76-0004 entitled "Aircraft Scale Model Measurements and Scaling Verifications" and presents the measured surface current and charges on model EC-135 aircraft simulated in the free space. For these measurements, topside incidence was always used and the incident wave had, depending upon a particular measurement, either symmetric (incident electric field parallel to the fuselage) or anti-symmetric polarization. The laboratory measurements were made in 1.0 to 4.0 GHZ frequency range which for 1/447 to 1/114 scale model aircraft used correspond to 2.3 MHz to 35 MHZ (full scale) frequencies. However, in this report data is presented only up to 20 MHz. Measurements are presented for models with and without attached HF wire antennas connected between the top of the fuselage (near cockpit) and the vertical stabilizer.

2. MEASUREMENTS

2.1 Facility and Equipment

The data presented herein was measured in our surface field measurement facility. The equipment and procedures used were essentially those described in AFWL-TR-75-217.* Figure 1 shows the basic block diagram of the facility, which, in turn, can be generalized in three basic groups, i.e.:

1. The anechoic chamber
2. The sweep r.f. source (sweep generator, power amplifier, isolator, and antenna), and
3. The receiving and recording equipment (sensors, preamplifier, phase shifter, network analyzer, analog X-Y recorder, and CRT display).

2.2 Models

For measurements presented here, seven models ranging in scale from 1/114 to 1/447 were used. They all were purchased as some versions of Boeing 707 models and when related to EC-135 dimensions they do not generally have the same length and

---

* Valdis V. Liepa, "Sweep Frequency Surface Field Measurements", University of Michigan Radiation Laboratory Report 013378-1-F. AFWL-TR-75-217, 1975.

MISSING
PAGE

wingspan scale. In translating the measurement frequencies to full scale frequencies the length scale factors were used for case of symmetric excitation and the wingspan scale factor used for the anti-symmetric excitation.

The refueling booms, cut out of wood, were added on all models; the booms as well as the entire non-metallic plane models were then spray painted with a conductive silver paint. Cockpit and fuselage windows were also painted and the landing gear doors and fuselage-wing joints (for metal models) were taped with conductive aluminum or copper tape. Table 1 presents relevant dimensions and other description of the models used.

On some models HF wire antennas were installed. These were made of No. 30 wire and installed per specifications as given in Figure 2. Note, both wires are electrically shorted at front but on the vertical stabilizer the upper one is shorted and the lower one is open. (The open circuit condition was obtained by using a section of string, approximately 1/16 inch long.)

2.3 Sensors

The measurements were made with so-called hard lead probes: the surface currents were measured using a bent 3.2 mm diameter shielded loop probe (c.f. Figure 18 of TR-75-217) and the charge measurements were made using an extension of the center conductor of a 0.020 inch diameter coax. This extension or monopole was typically 0.060 inches and the cable was always brought to the surface from within the model. For the charge measurements on the nose of the aircraft, a hole in a model was drilled from nose (STA: F130)** into the front landing gear cavity. The sensor lead was then brought out from there and taped along the belly of the plane up to STA: F800B from where it was removed in a direction normal to fuselage and parallel to the direction of propagation of the incident wave. In the case of the wingtip charge measurements at STA: W940T the cable again joined the model at STA: F800B from where it was taped along the underside of the wing and passed to the top through a 0.025 inch diameter hole drilled through the wing.

** The locations of body station numbers are given in Figure 3. The letter F (or W) in front of the number refers to fuselage (or wing) location, while the T (or B) after the number designates the top (or the botton) of the aircraft.

TABLE 1 : EC-135 Models Used

EC-135 Model	Fuselage Scale	Wing Span Scale	Material	Fuselage Height at Station			Wing Thickness at W600	With HF Wires	Without HF Wires
				400	800	1200			
447	1/447	1/466	metal	0.93 cm	0.94 cm	0.86 cm	.17 cm	X	X
325	1/325	1/341	metal	1.15	1.19	1.15	.23	X	X
224	1/224	1/225	metal	1.80	1.77	1.76	.28	X	
129	1/129	1/134	plastic	3.01	3.03	3.02	.59		X
114	1/114	1/117	plastic	3.50	3.44	3.35	.30	X	

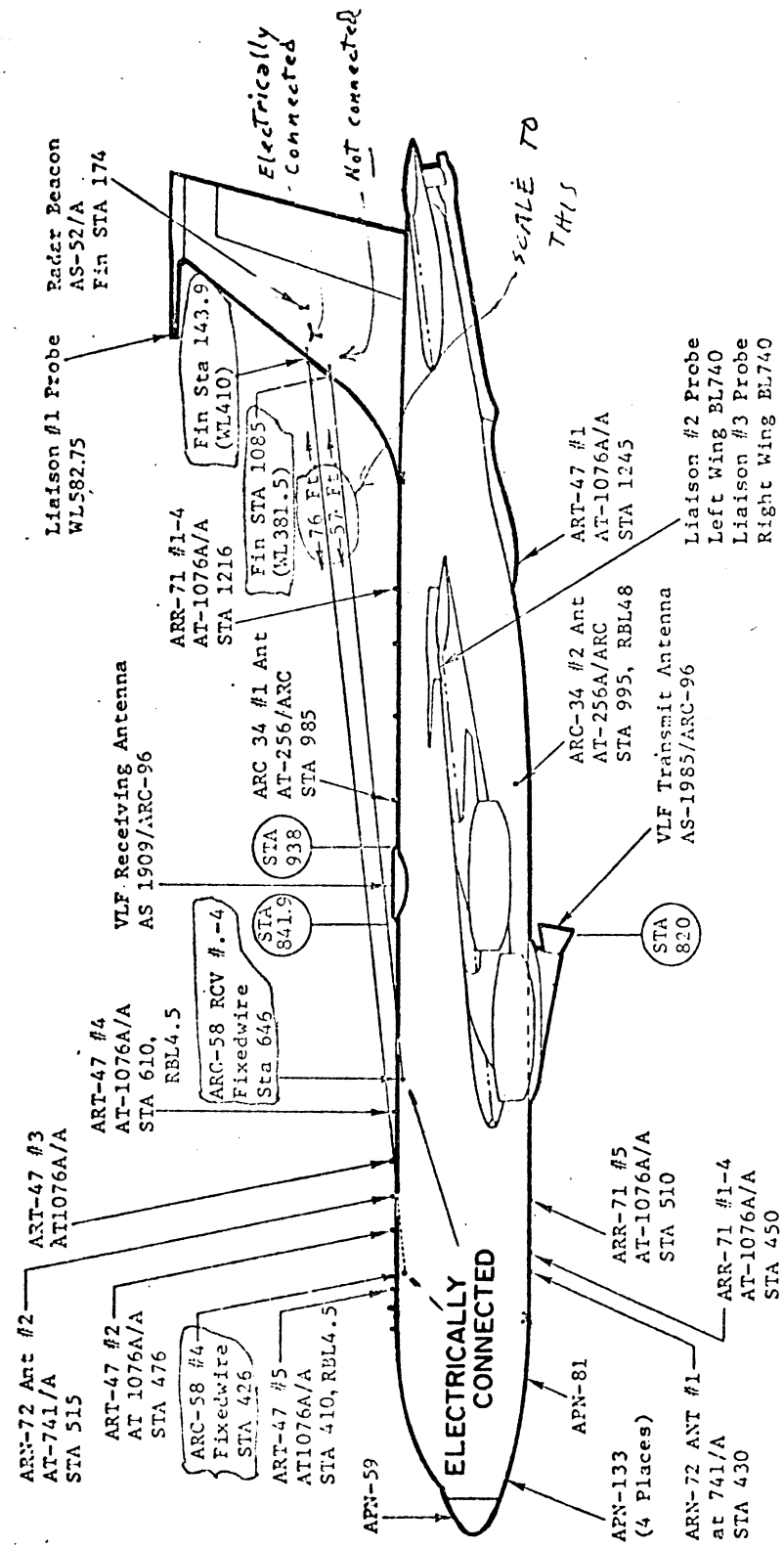

Figure 2: EC-135 HF Wire Antenna Installations

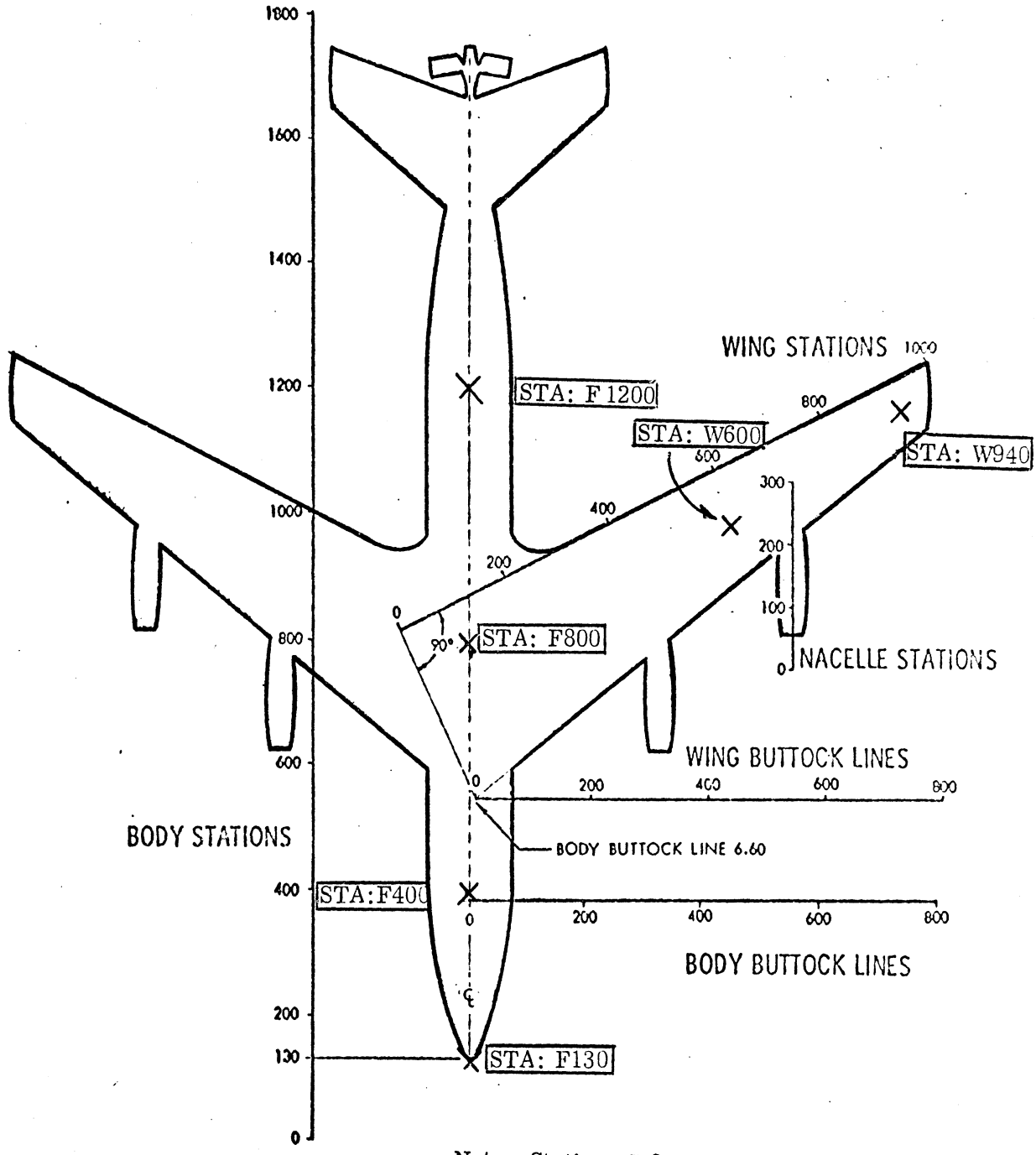

Note: Stations W600 and W940 are at mid-sections of the wing. Station W940 is located at the center of a circle tangent to the three wing edger.

Figure 3: EC-135 Aircraft Body Stations;
X Designates Measurement Locations

For current measurements an external B-dot sensor or current loop probe was used. It touched the model only at the point of measurement and even there it was separated by a small dielectric epoxy bead. Since the incident field was always horizontally polarized, the incident electric vector was always perpendicular to the sensor lead thus providing minimal interactions with the incident field.

2.4 Reduction of data

When current or charge data for a given frequency scan is recorded on graph paper by X-Y recorder, it shows only very slight resemblance to what one would expect for the given case. Due to non-uniform frequency response of the measurement facility the raw data must first be normalized to the incident field which is obtained by measuring the corresponding field with the same sensor on a 3.133 inch and/or 6.0 inch diameter sphere(s). Data is read off from these curves typically at 100 MHz intervals (recall measurements are made in 1 - 4 GHz range) and reduced manually using an electronic pocket calculator and a sharp pencil. Where applicable, corrections for probe integration effects for current and charge measurements are applied.

These corrections have maximum effect on the smaller scale models where, in certain cases, current amplitude is increased by as much as 33 percent and charge by 60 percent.

3. DATA

The measured surface current and charge data normalized to full scale frequencies are presented in figures 4 through 27. When amplitude and phase data are presented, Figure XXa contains amplitude data while Figure XXb contains corresponding phase data. This data is relative to the phase of the incident field at the particular measurement stations. Also it will be helpful to note that the even figure numbers contain data for models without HF wire antennas, while the odd figures contain data for models with HF wire antennas.

Table 2 summarizes the data presented. Its main purpose is to provide a selection guide to find quickly a particular data. For example, if needed a current

amplitude on top of the fuselage, with HF wires, station 800, anti-symmetric excitation — go to line designated F800T (Fuselage, 800, Top) and then across the table to select the appropriate case. In this case it would be Figure 23a.

The graphs presented should be self-explanatory. The sketch insert in the upper hand corner gives immediate information on incidence, incident polarization, and the measurement location. The field values are relative to the incident field and are plotted on a linear scale. Many figures have two or even three curves over the same frequency range. Such data overlapping resulted when different scale models were measured over extended frequency range, and since each represents a different and independent measurement, the spread of data values should be indicative of the measurement accuracy for the particular body station and frequency.

TABLE 2: Data Selection Chart

Station Number	EC-135 without HF wires				EC-135 with HF wires			
	Symmetric		Anti-Symmetric		Symmetric		Anti-Symmetric	
	J	Q	J	Q	J	Q	J	Q
F400T	4a, b				5a, b			
F800T	6a, b		22a, b		7a, b		23a, b	
F1200T	8a, b				9a, b			
F400B	10				11			
F800B	12		24		13		25	
F1200B	14				15			
W600T			18a, b				19a, b	
W600B			20				21	
F130		16				17		
W940T				26				27

Note: When Figures a and b are specified, a designates amplitude and b designates phase. Otherwise, only amplitude is presented.

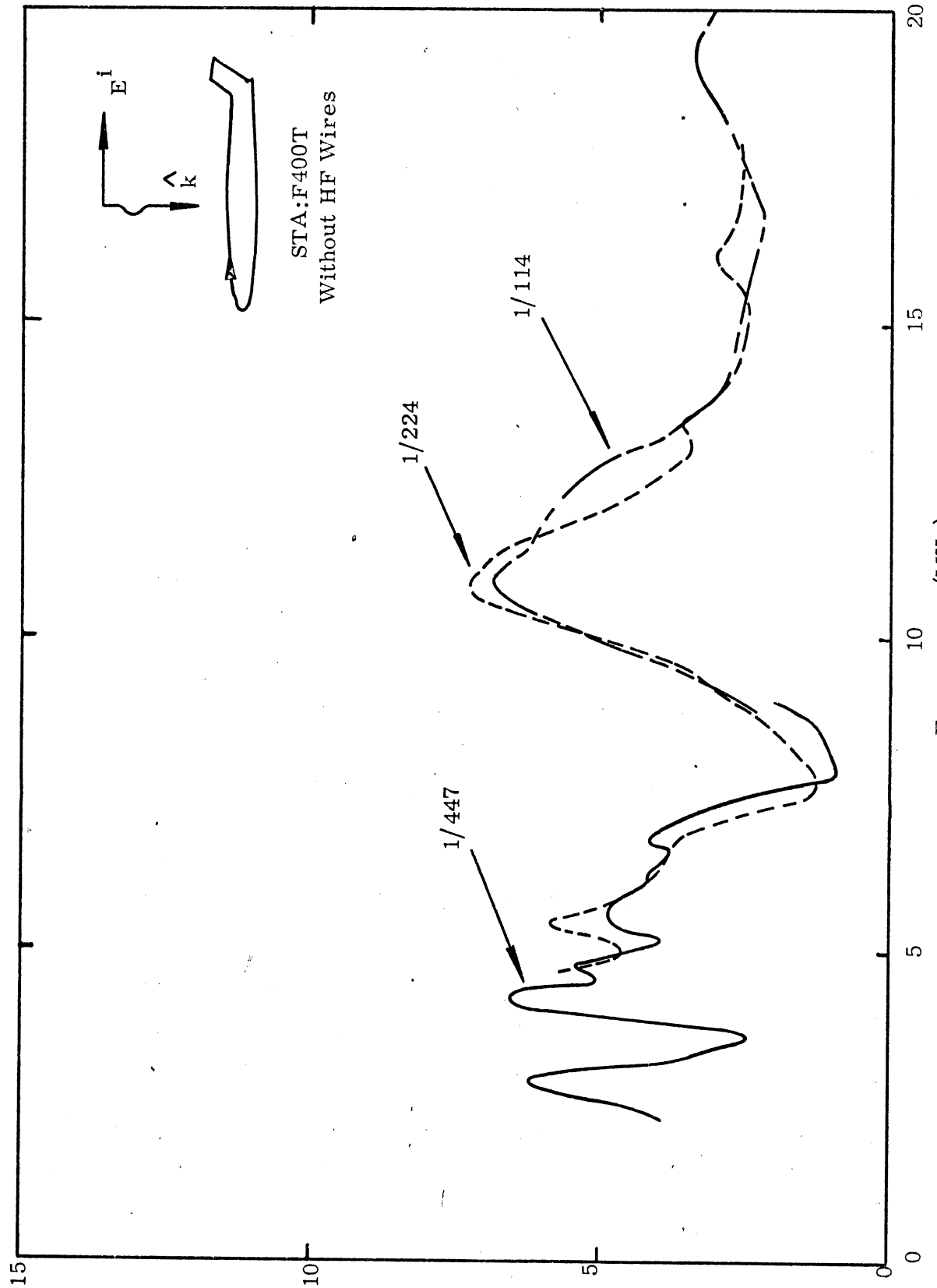

Figure 4a: Current Density at STA:F400T, Symmetric Excitation, without HF Wires

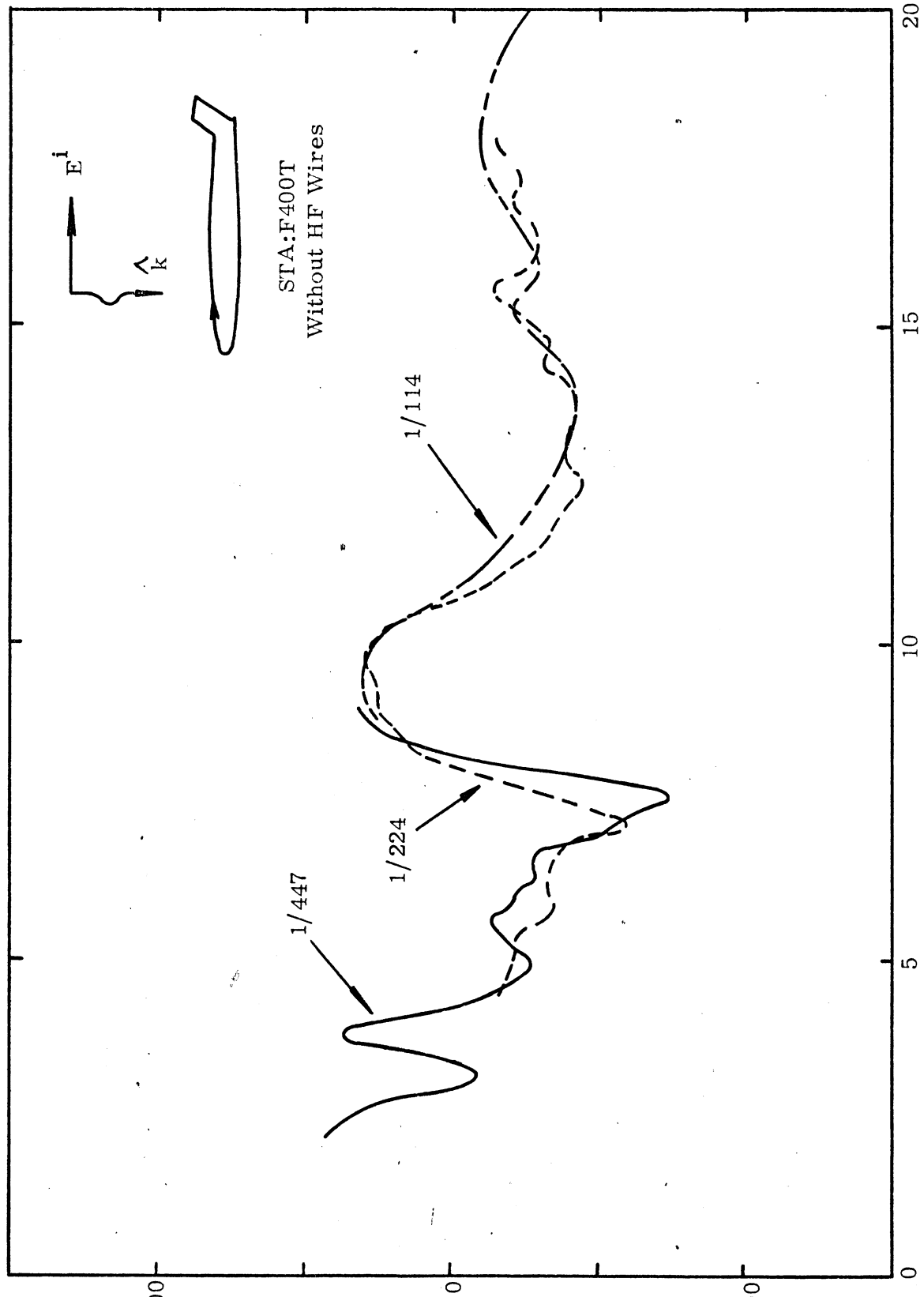

Figure 4b: Current Phase at STA:F400T, Symmetric Excitation, without HF Wires

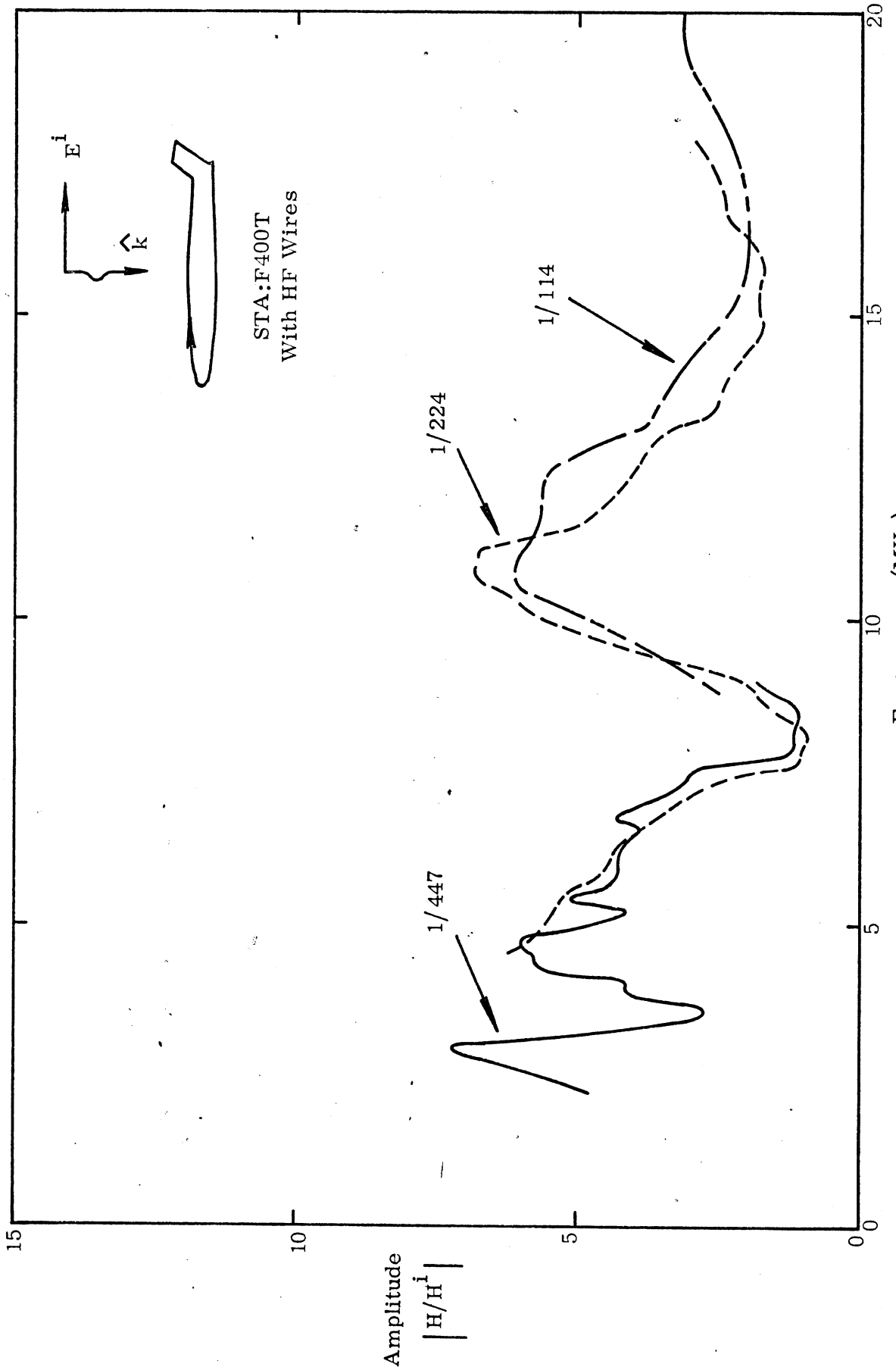

Figure 5a: Current Density at STA:F400T, Symmetric Excitation, with HF Wires

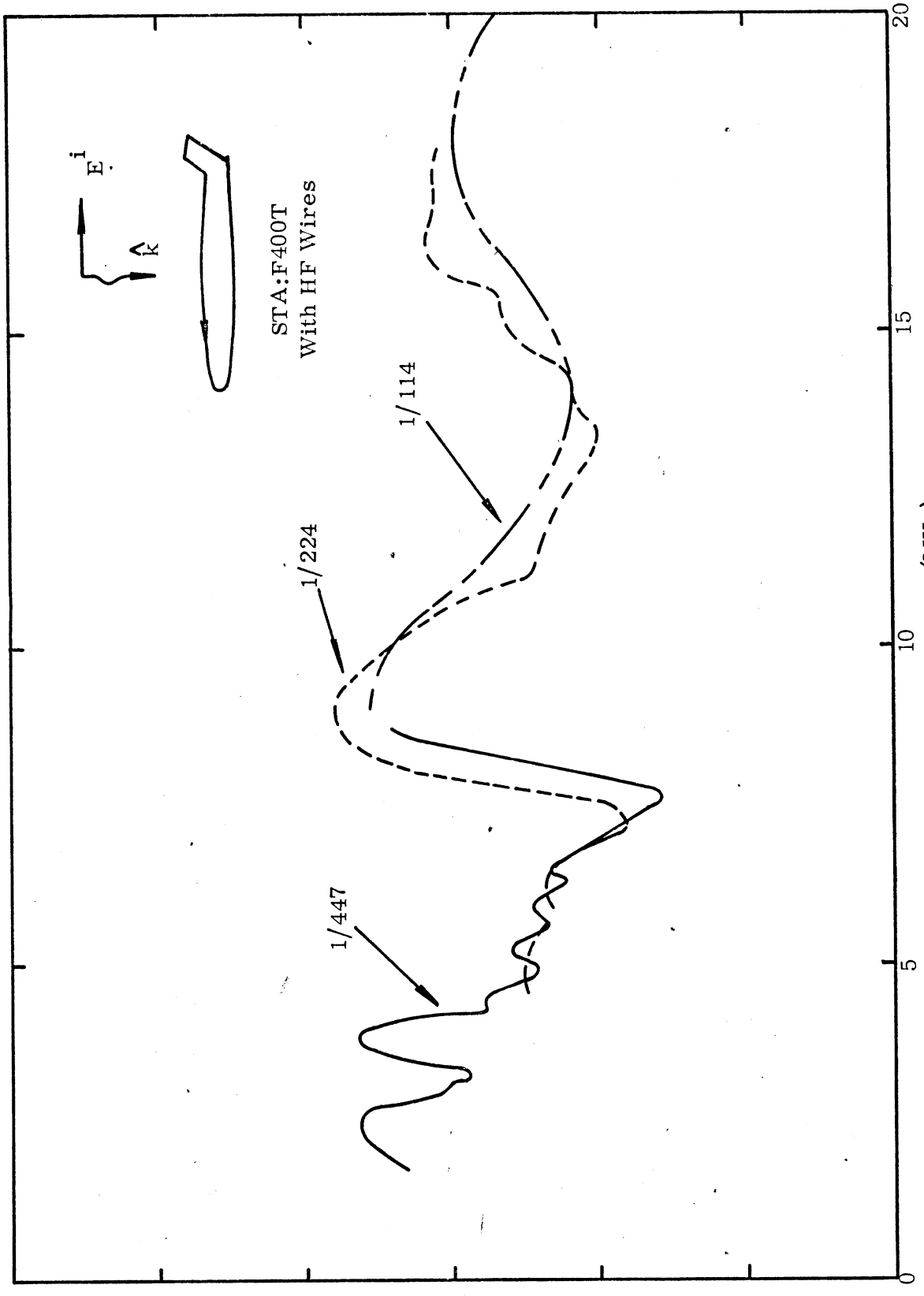

Figure 5b: Current Phase at STA:F400T, Symmetric Excitation, with HF Wires

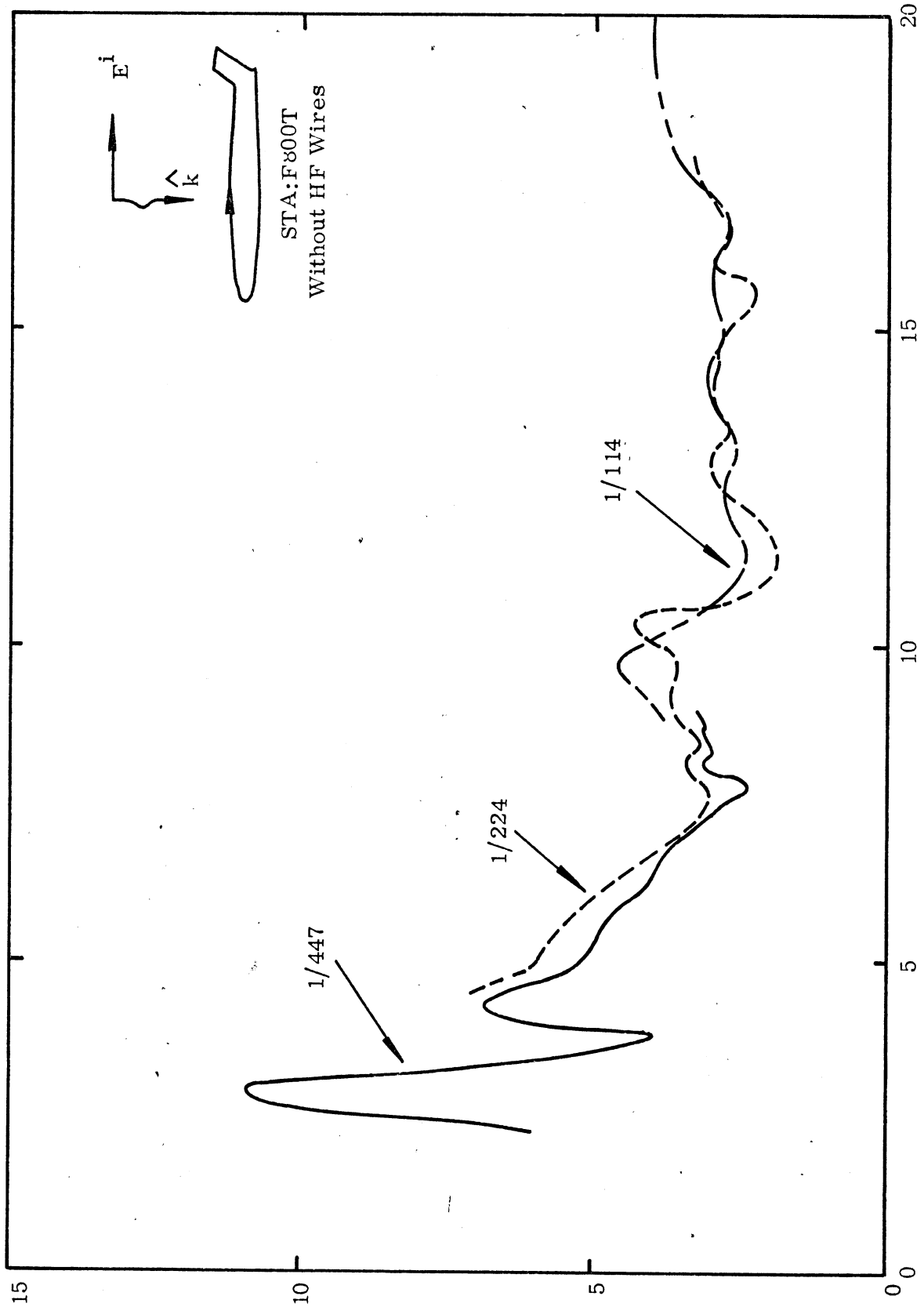

Figure 6a: Current Density at STA:F800T, Symmetric Excitation, without HF Wires

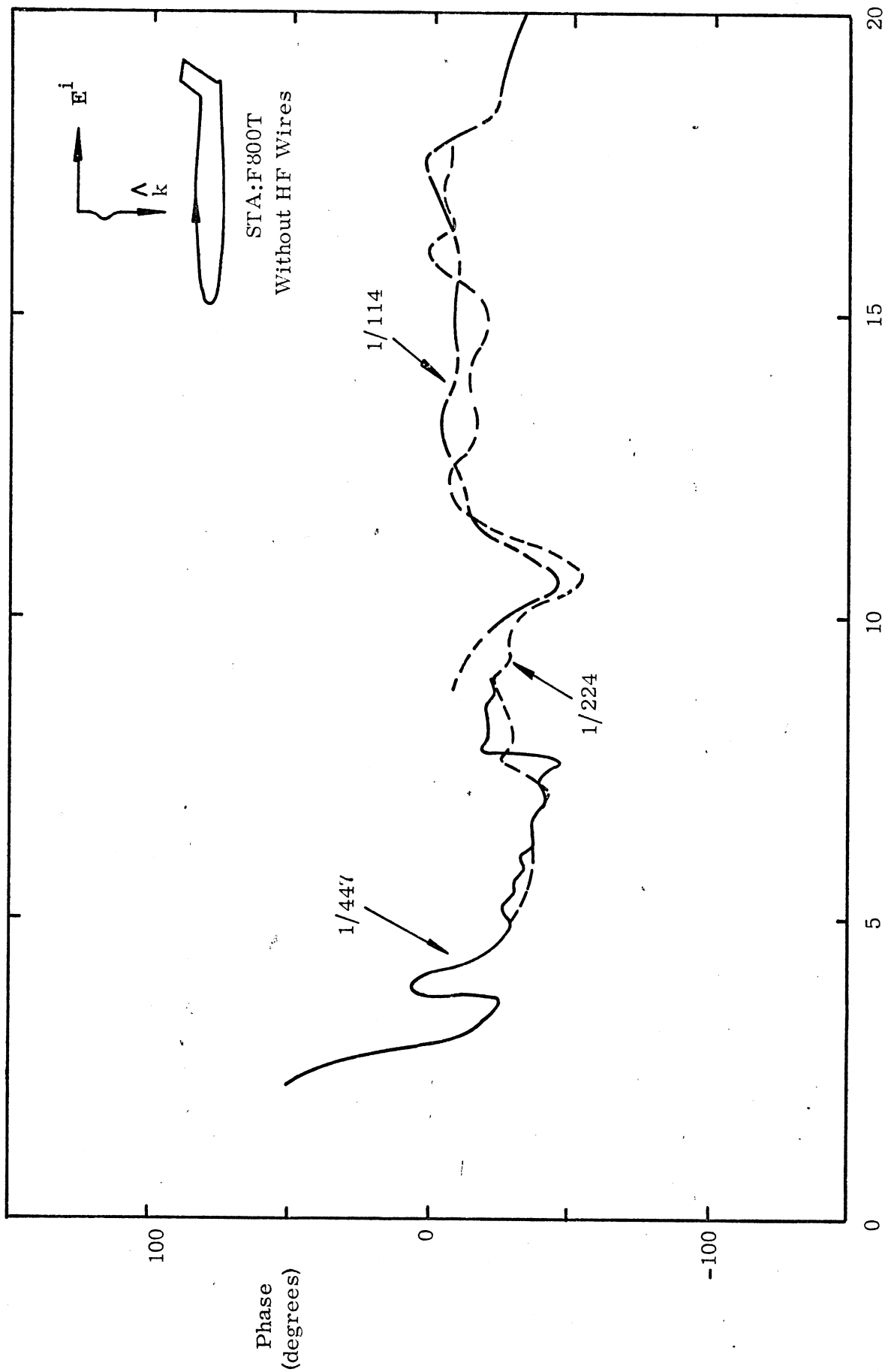

Figure 6b: Current Phase at STA:F800T, Symmetric Excitation, without HF Wires

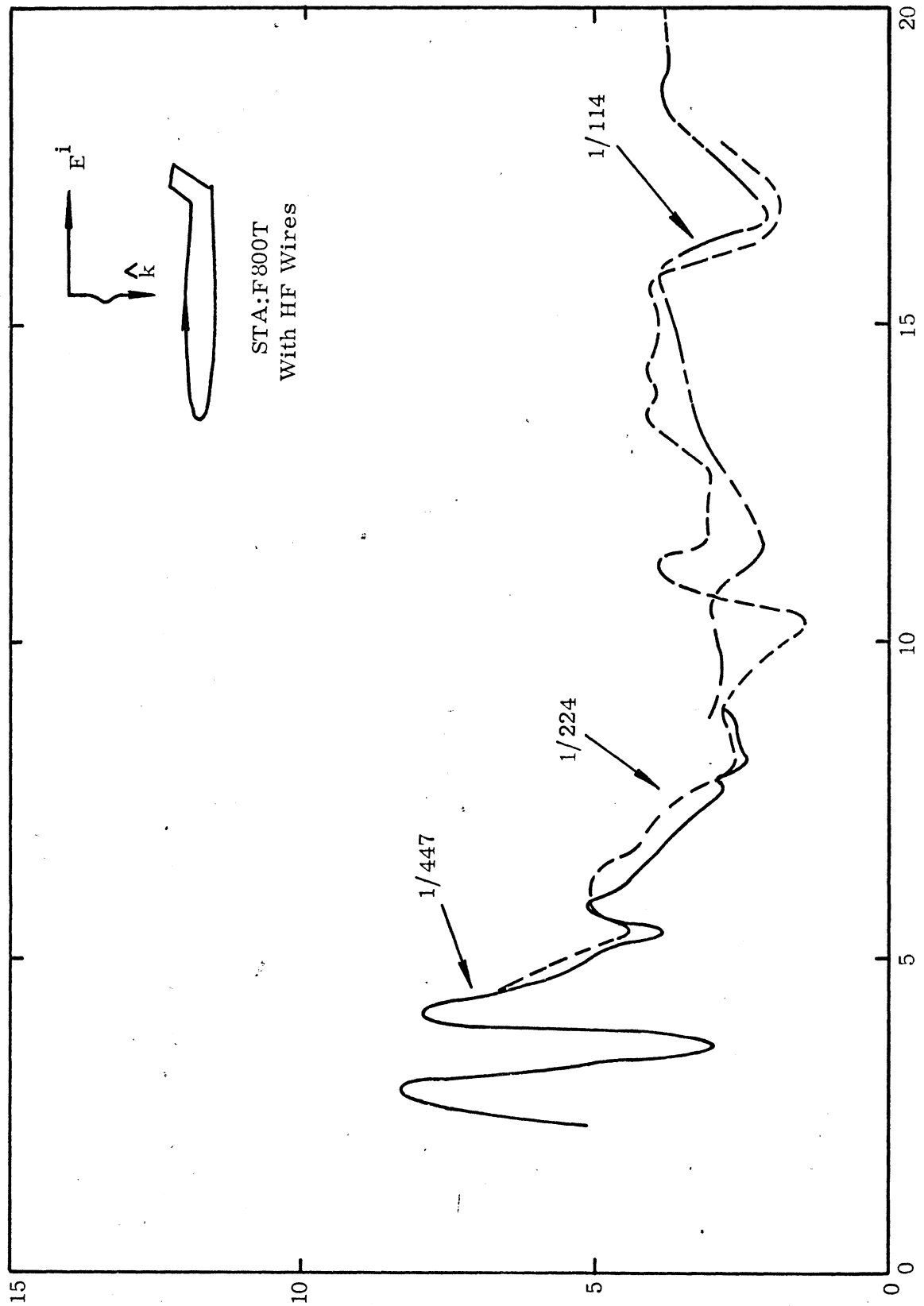

Figure 7a: Current Density at STA:F800T, Symmetric Excitation, with HF Wires

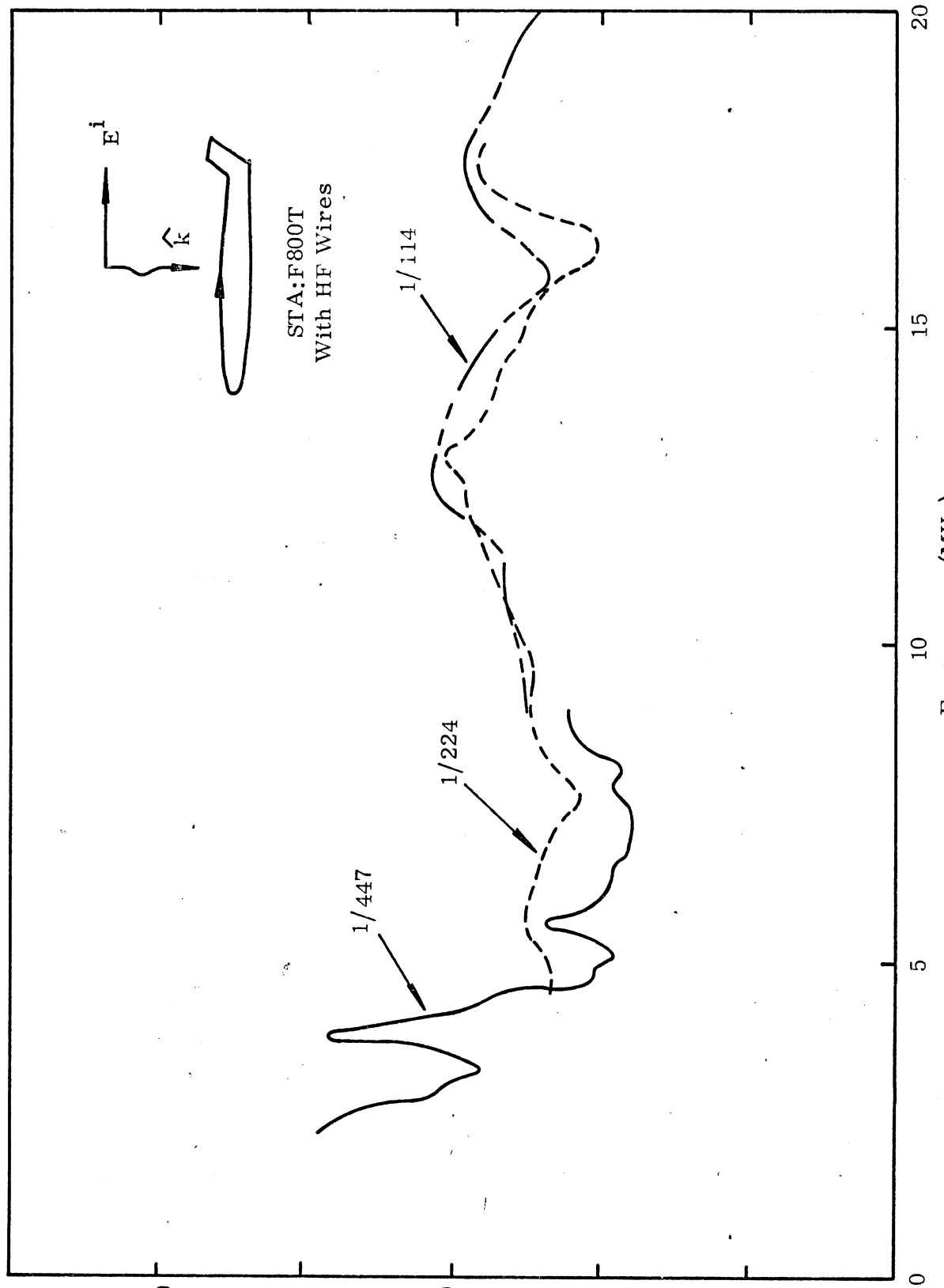

Figure 7b: Current Phase at STA:F800T, Symmetric Excitation, with HF Wires

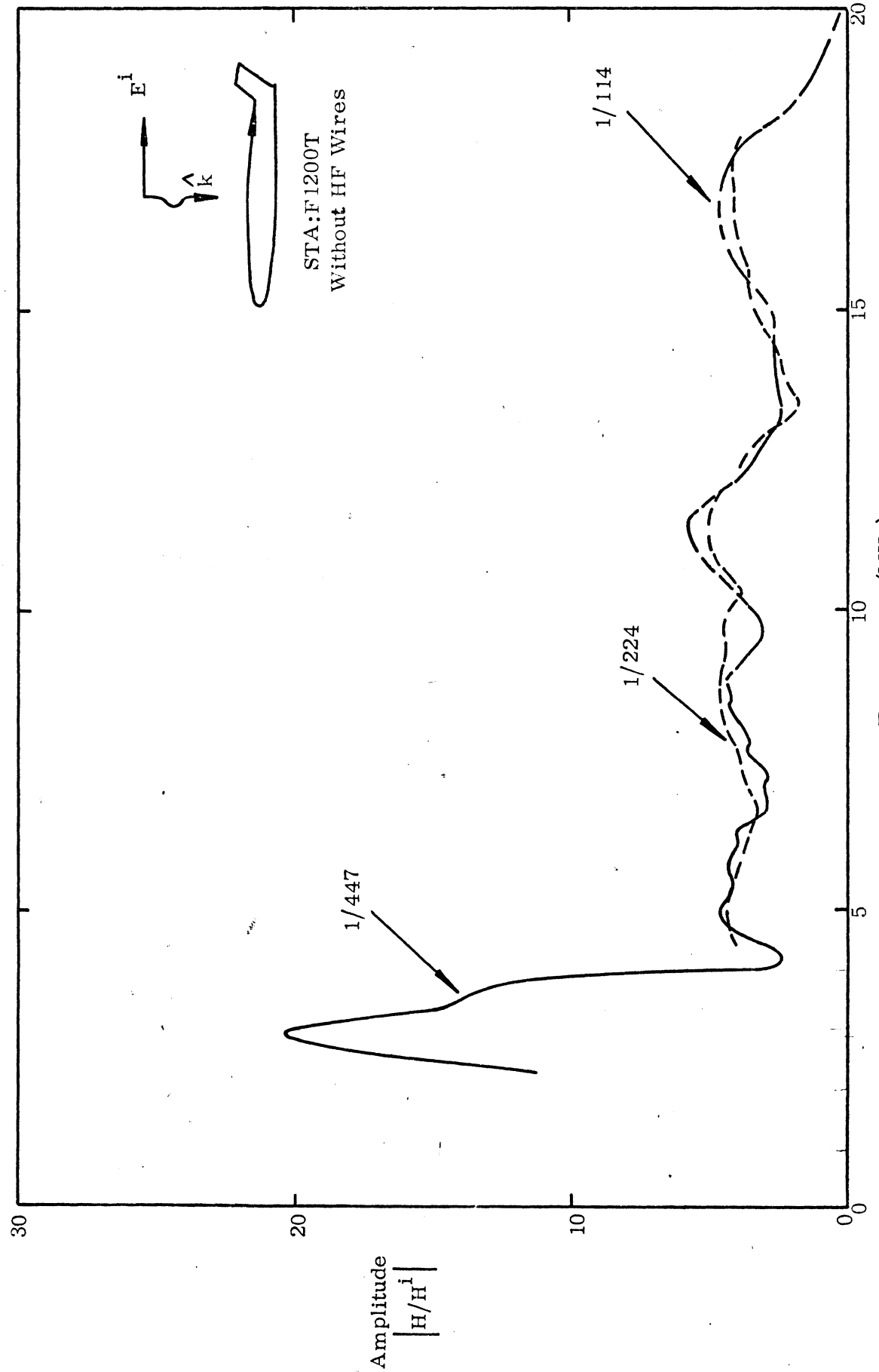

Figure 8a: Current Density at STA:F1200T, Symmetric Excitation, without HF Wires

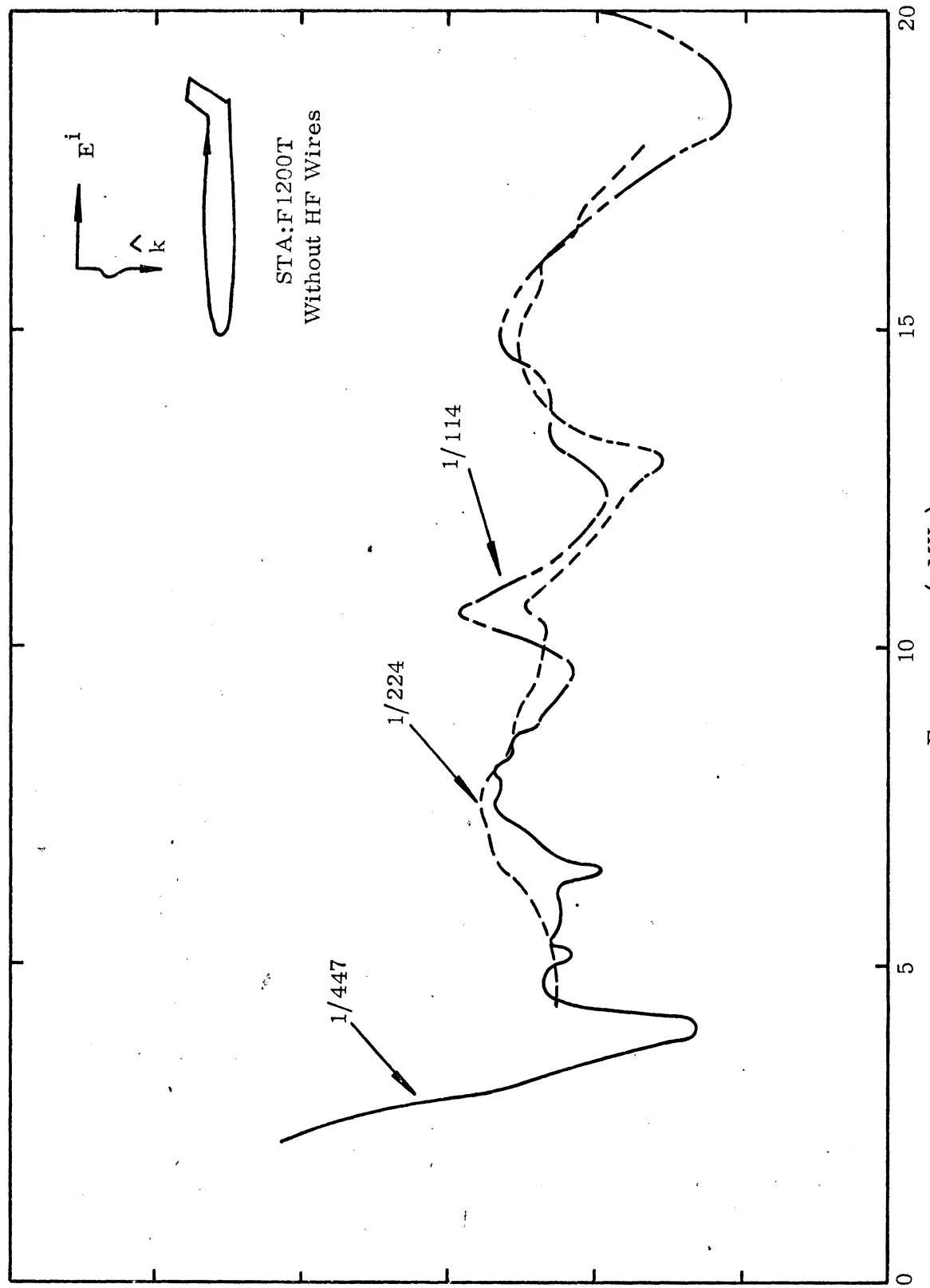

Figure 8b: Current Phase at STA:F1200T, Symmetric Excitation, without HF Wires

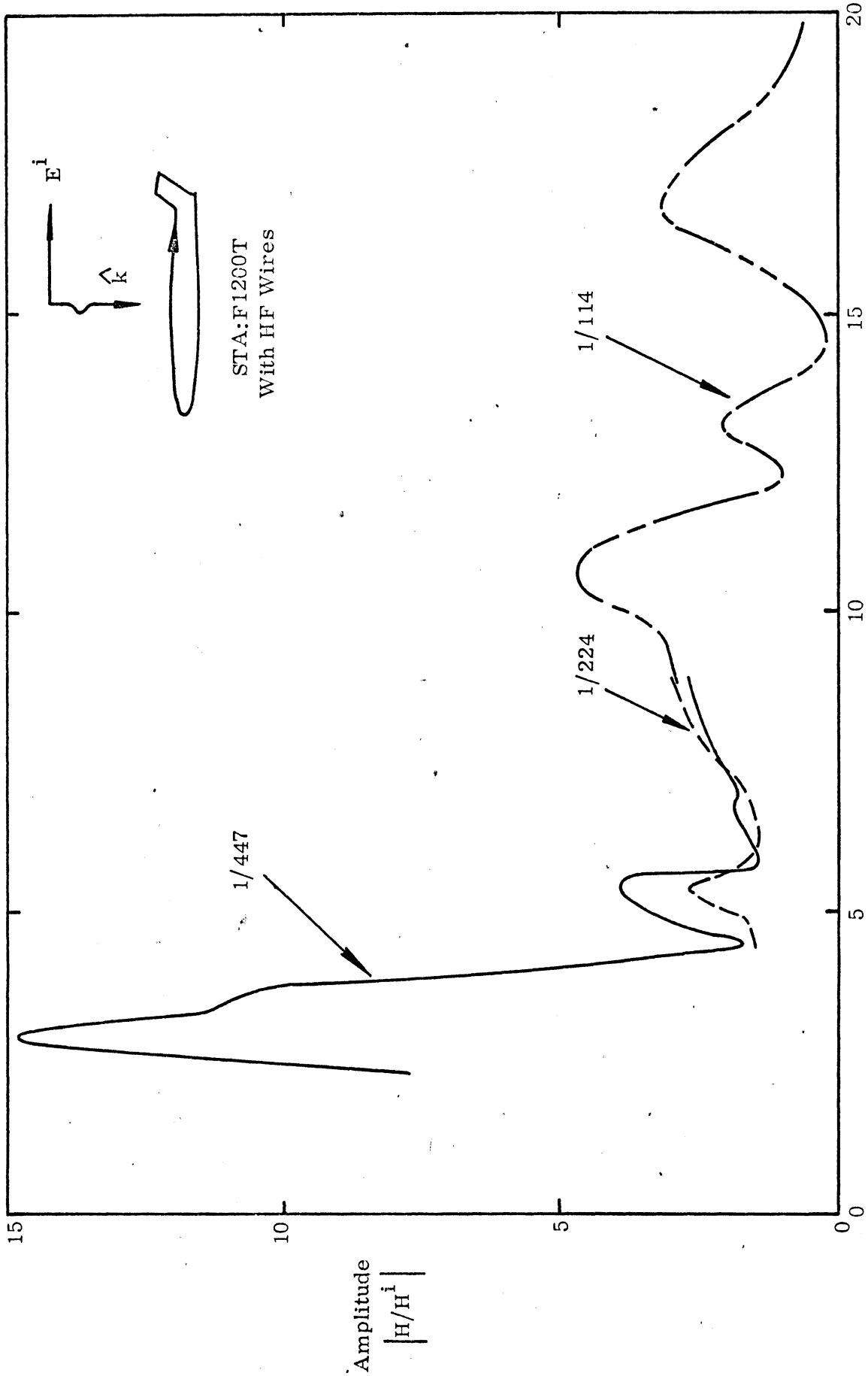

Figure 9a: Current Density at STA:F1200T, Symmetric Excitation, with HF Wires

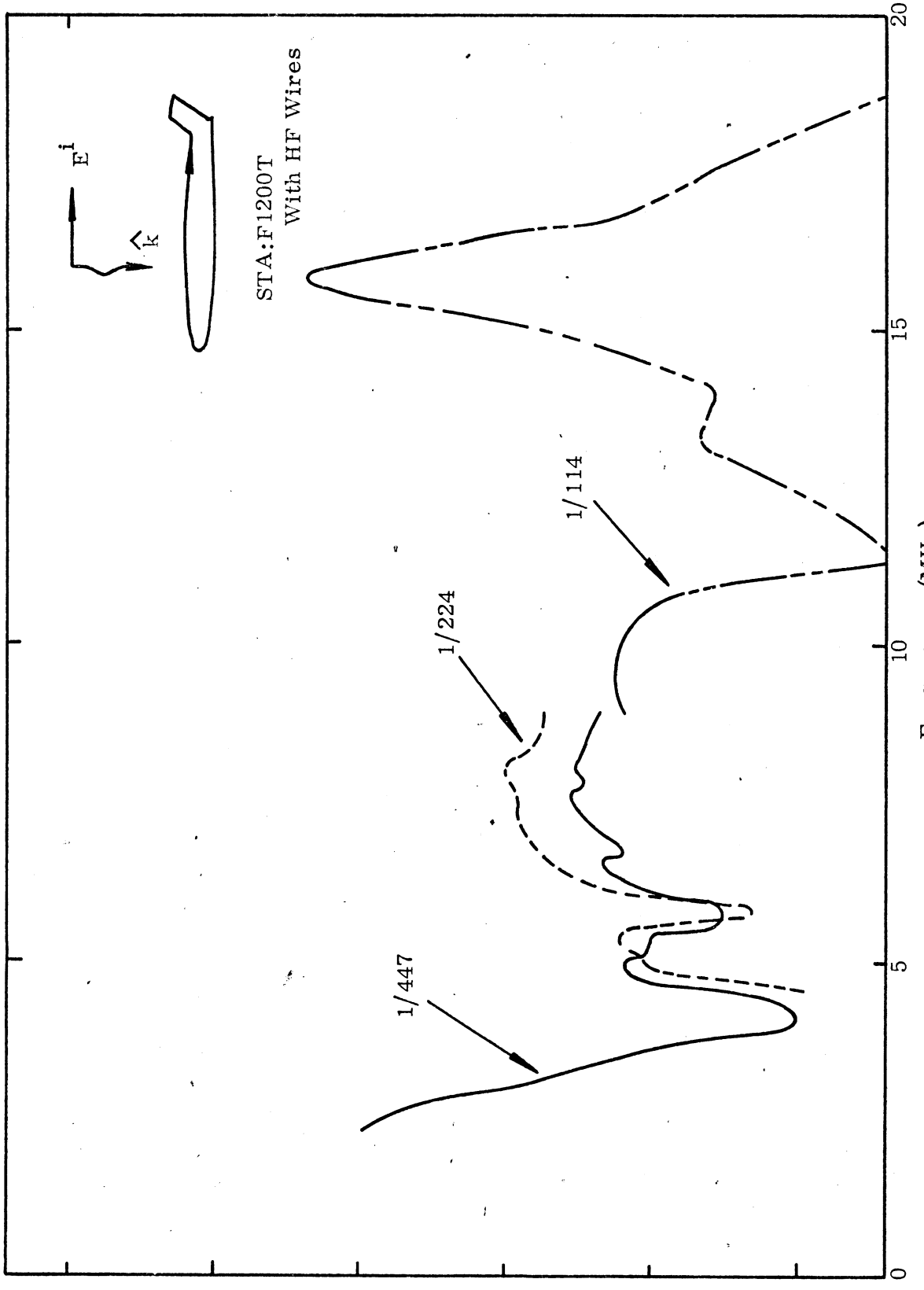

Figure 9b: Current Phase at STA:F1200T, Symmetric Excitation, with HF Wires

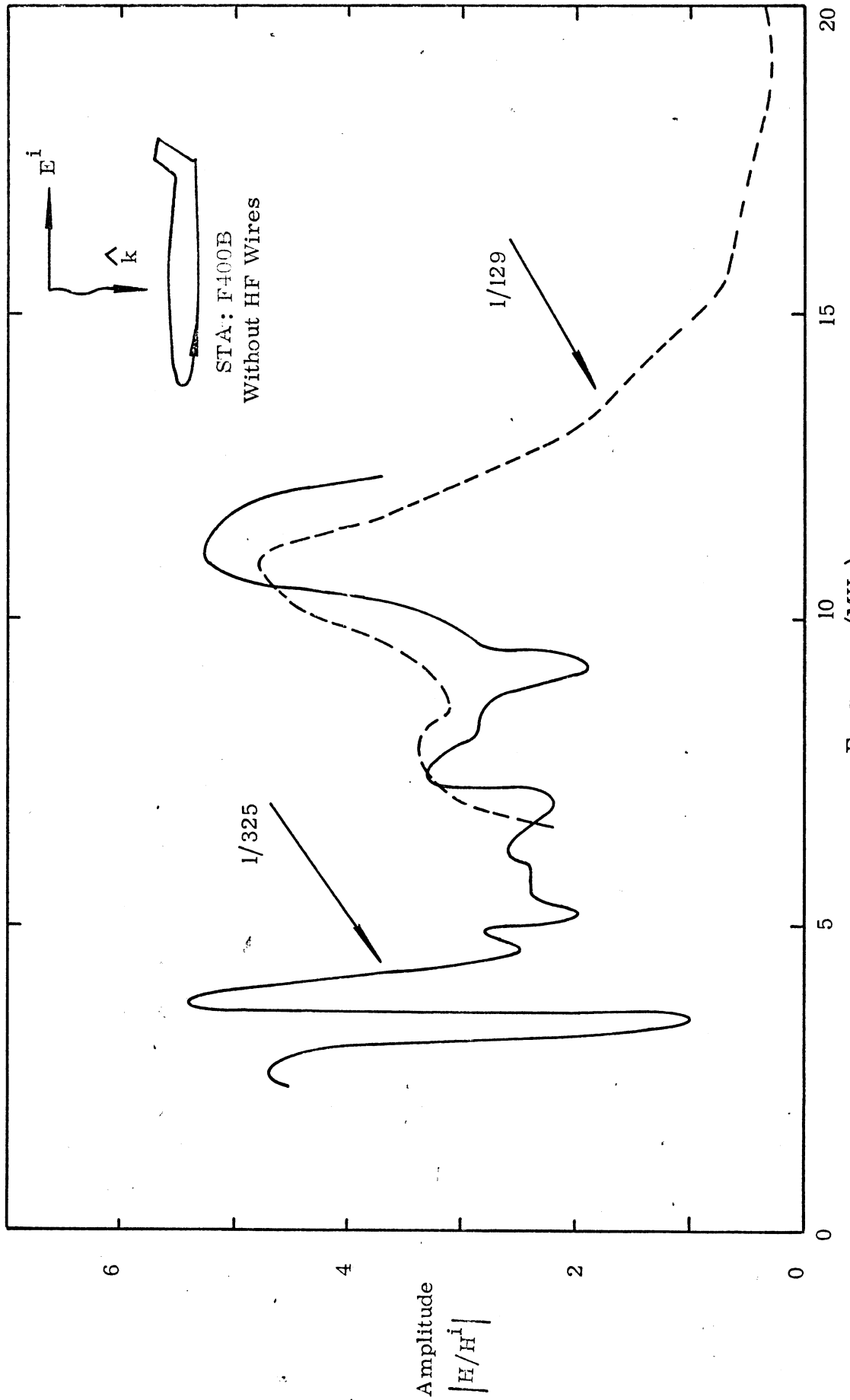

Figure 10: Current Density at STA: F400B, Without HF Wires, Symmetric Excitation

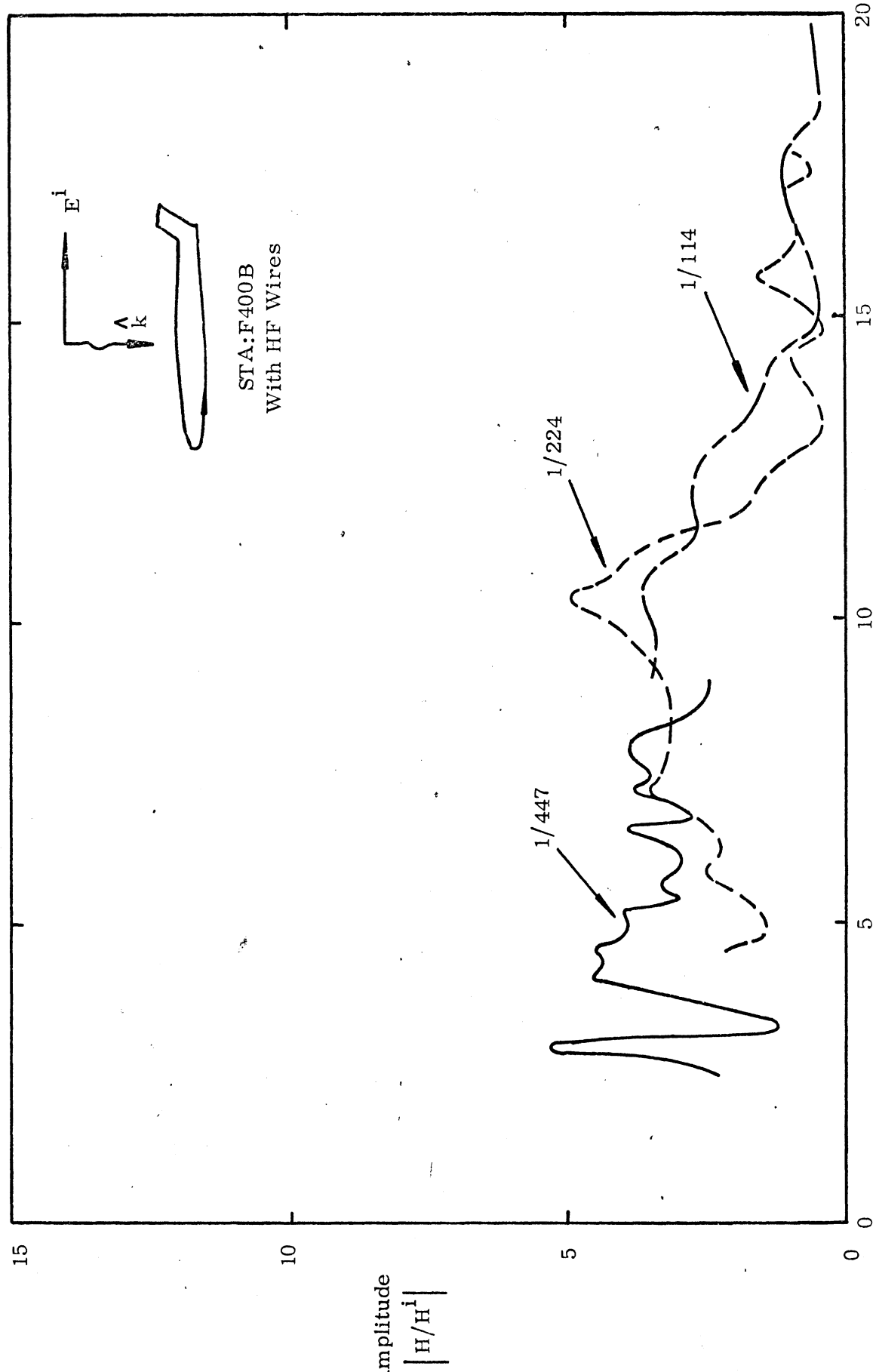

Figure 11: Current Density at STA:F400B, Symmetric Excitation, with HF Wires

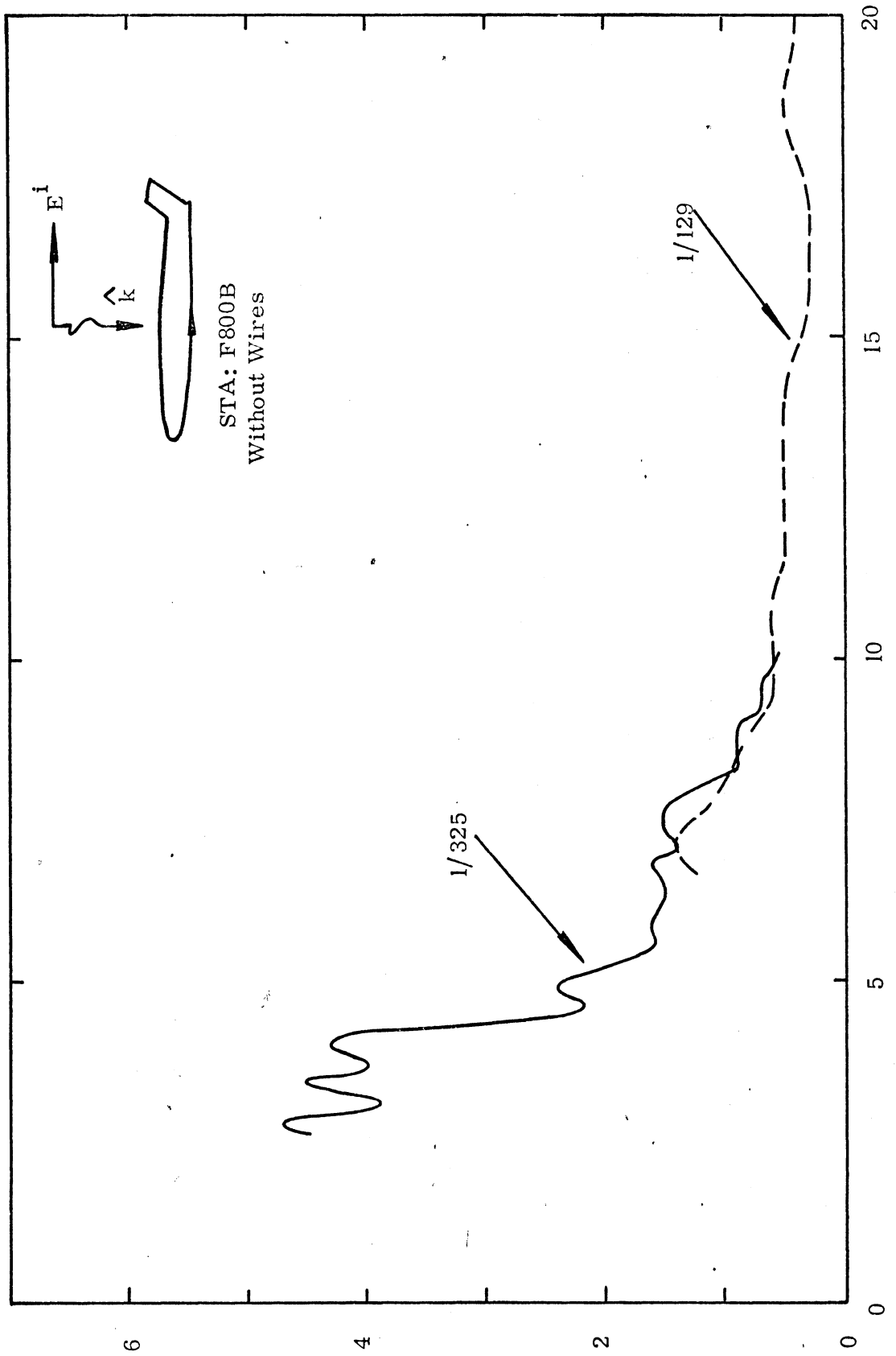

Figure 12: Current Density at STA: F800B, Without HF Wires, Symmetric Excitation

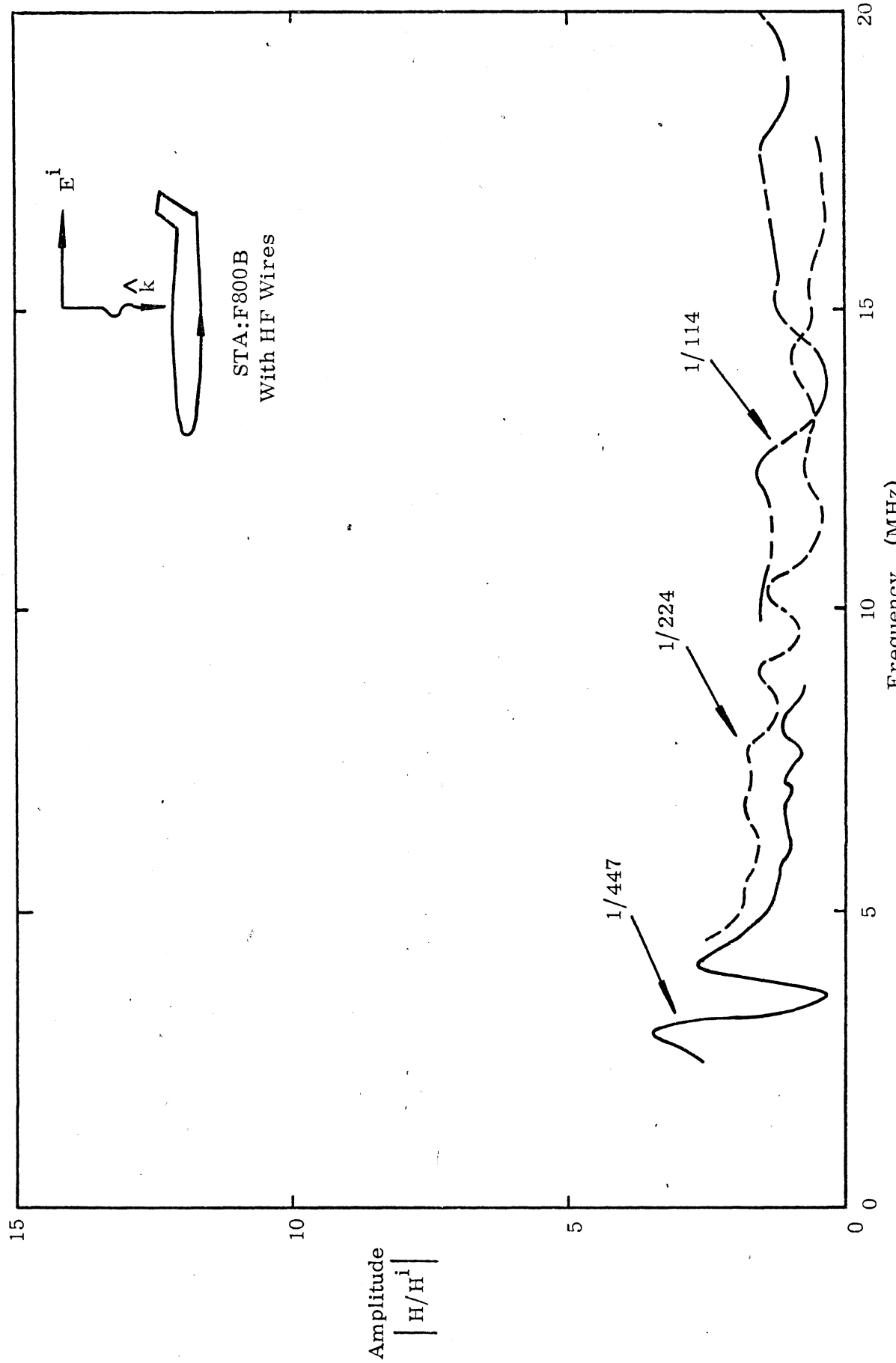

Figure 13: Current Density at STA:F800B, Symmetric Excitation, with HF Wires

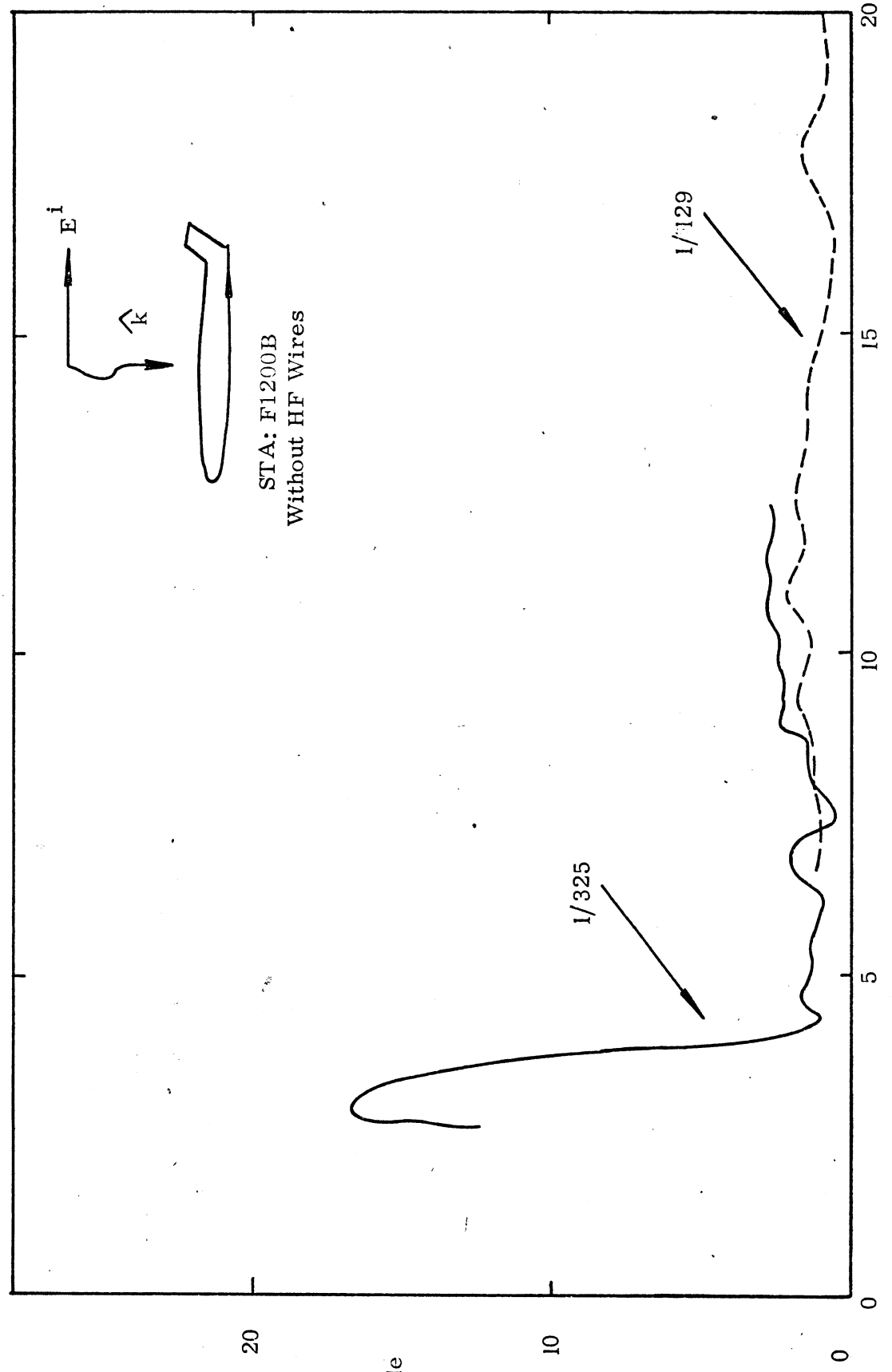

Figure 14: Current Density at STA: F1200B, Without HF Wires, Symmetric Excitation

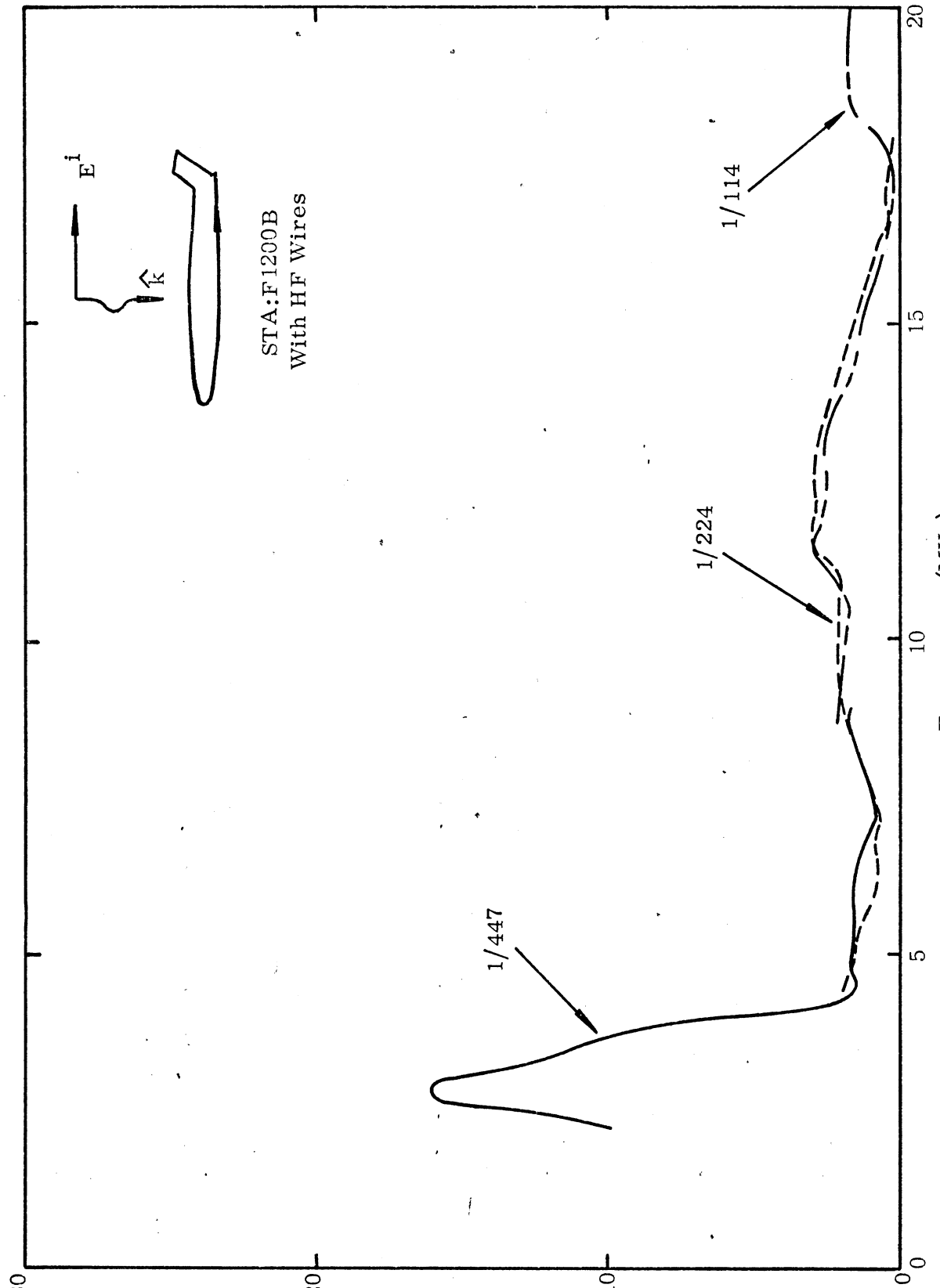

Figure 15: Current Density at STA:F1200B, Symmetric Excitation, with HF Wires

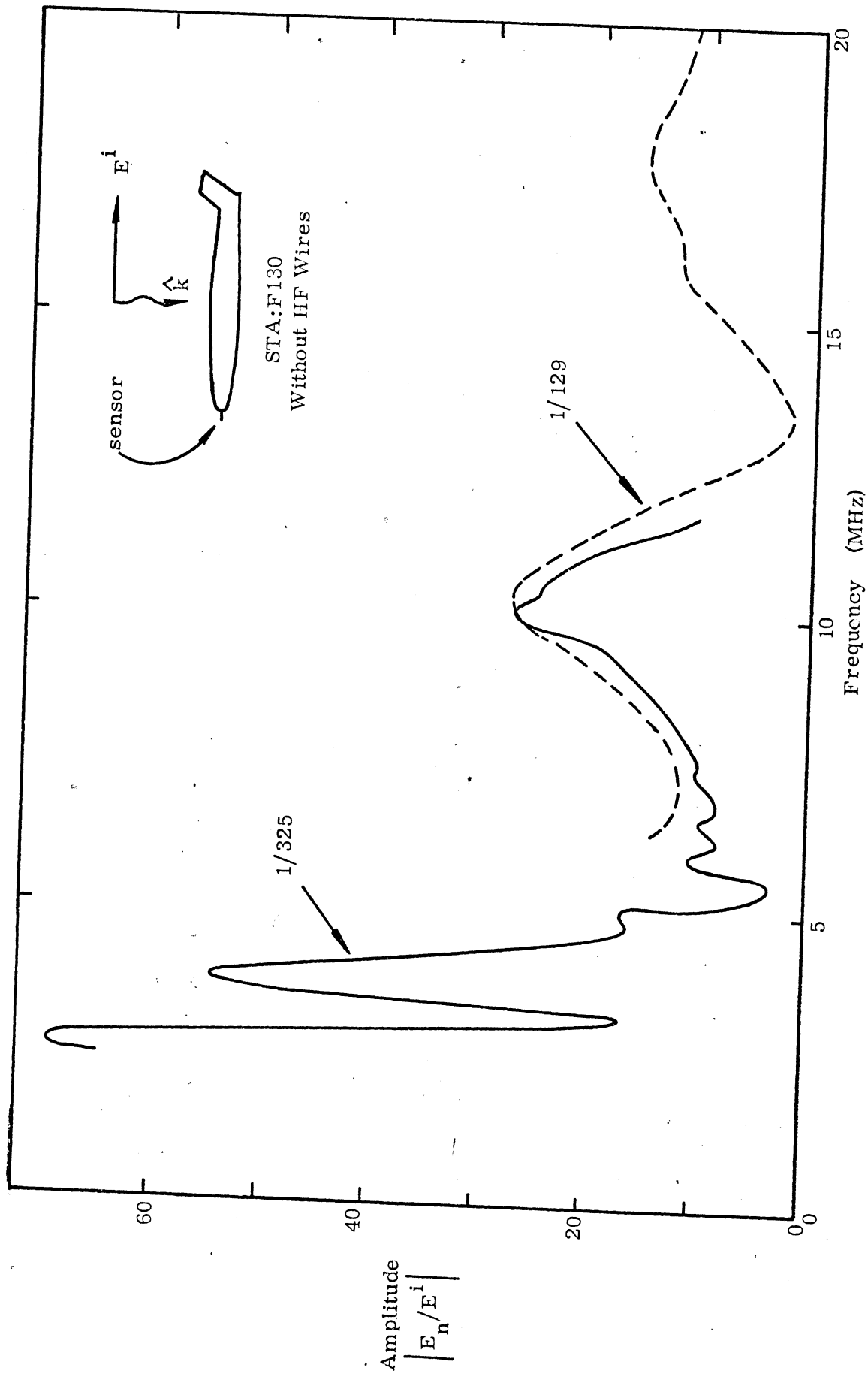

Figure 16: Charge Density at STA:F130, Symmetric Excitation, without HF Wires

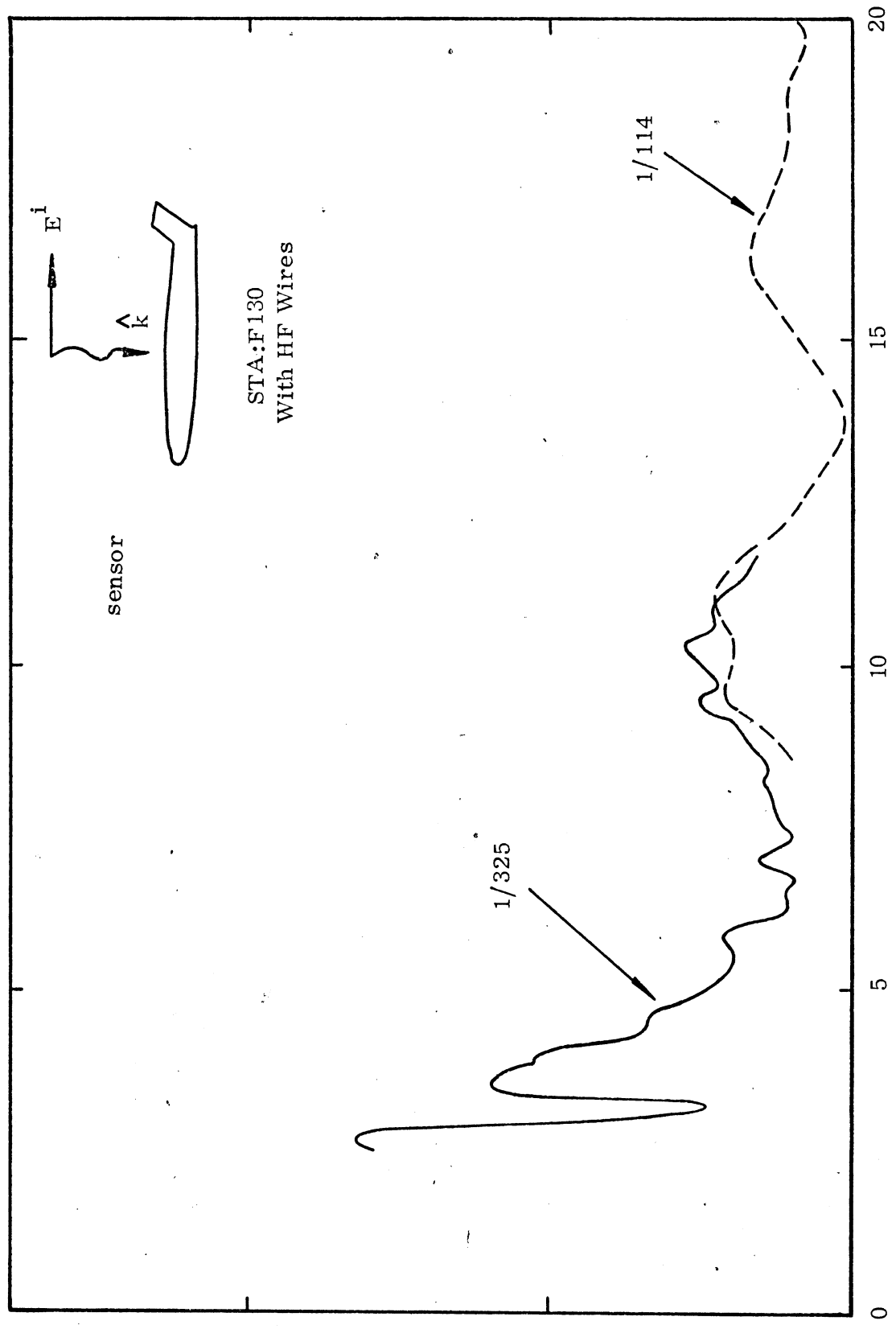

Figure 17: Charge Density at STA:F130, Symmetric Excitation, With HF Wires

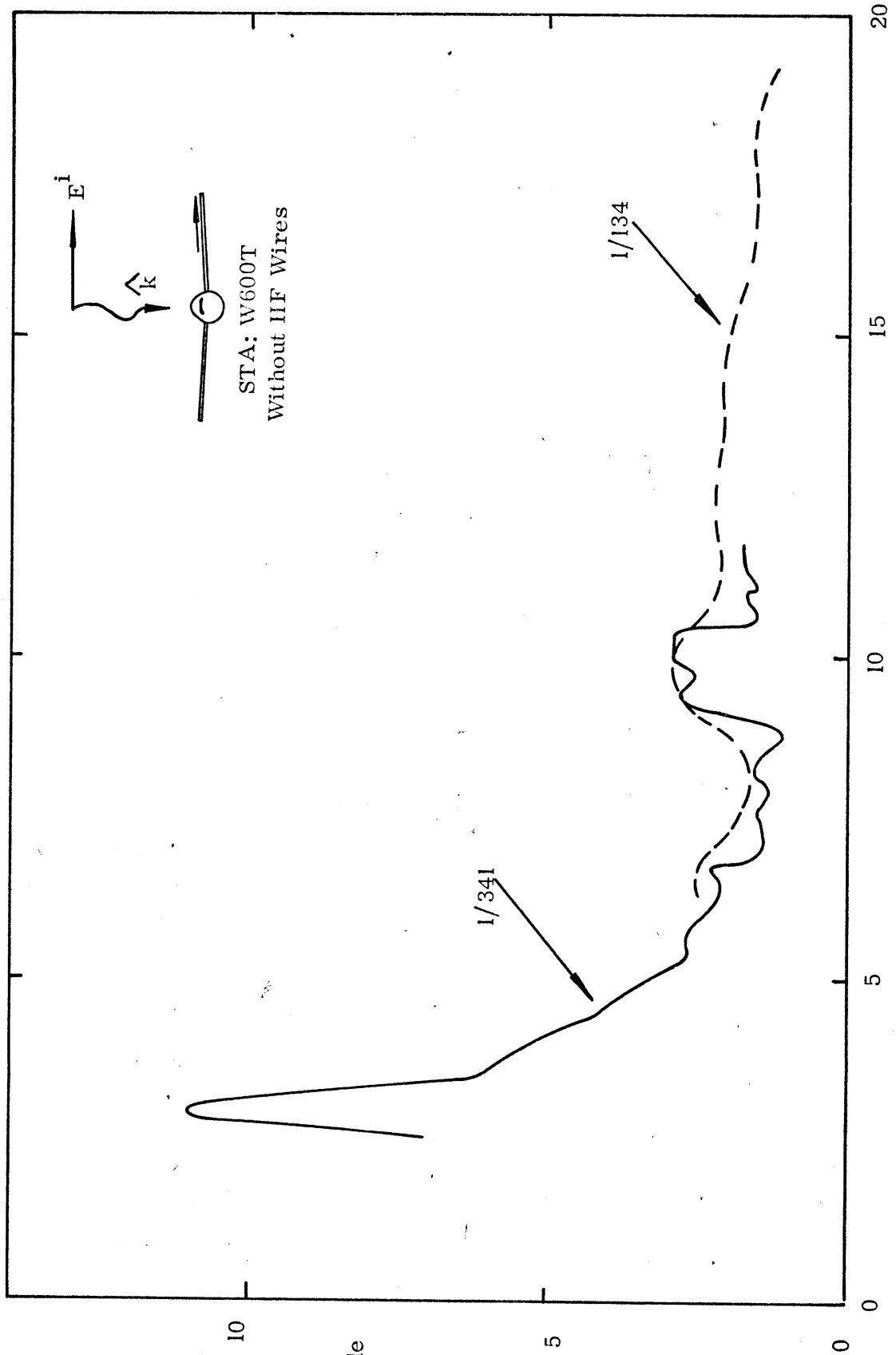

Figure 18a: Current Density At STA: W600T, Without HF Wires, Anti-symmetric Excitation

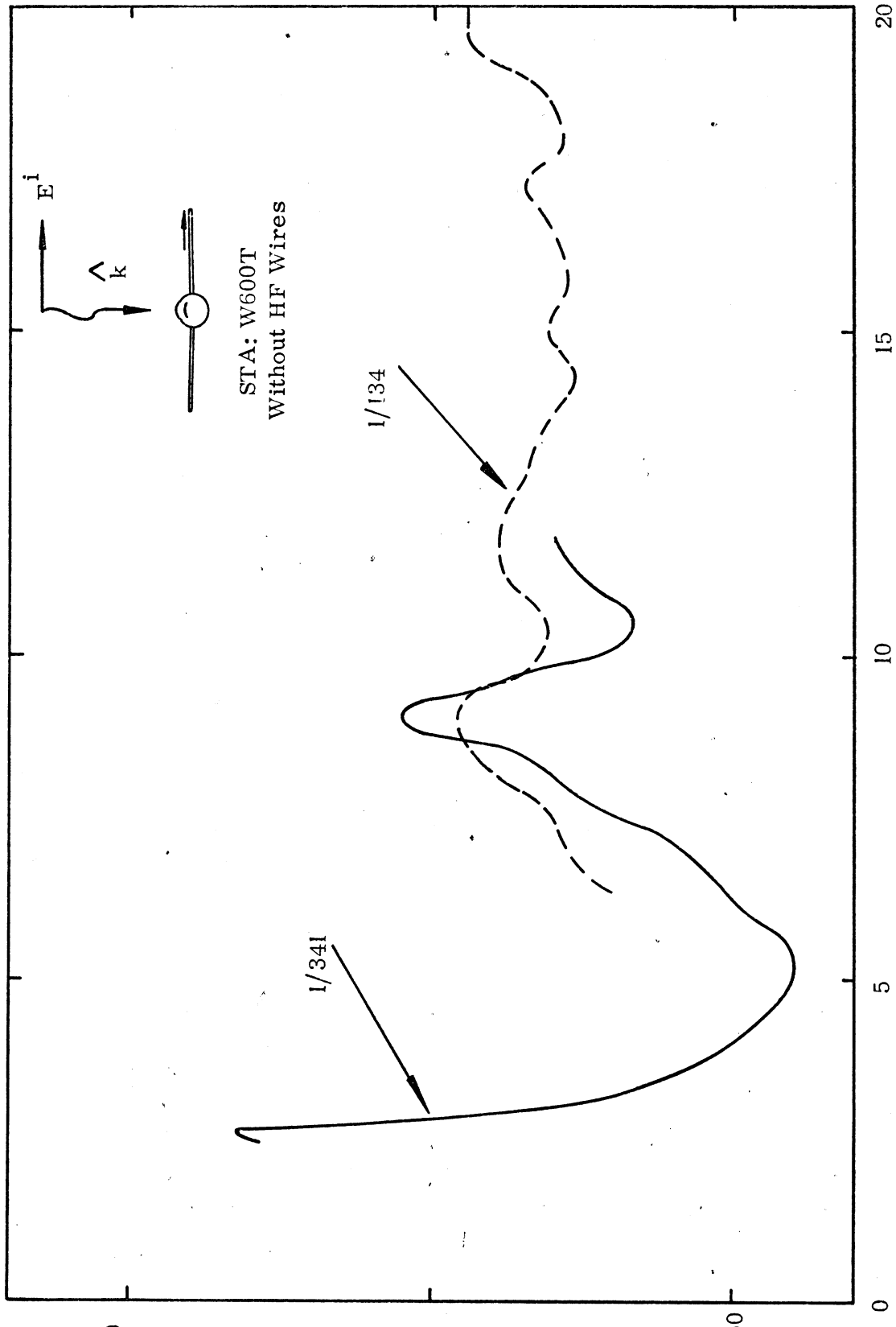

Figure 18b: Current Phase at STA: W600T, Without HF Wires, Anti-symmetric Excitation

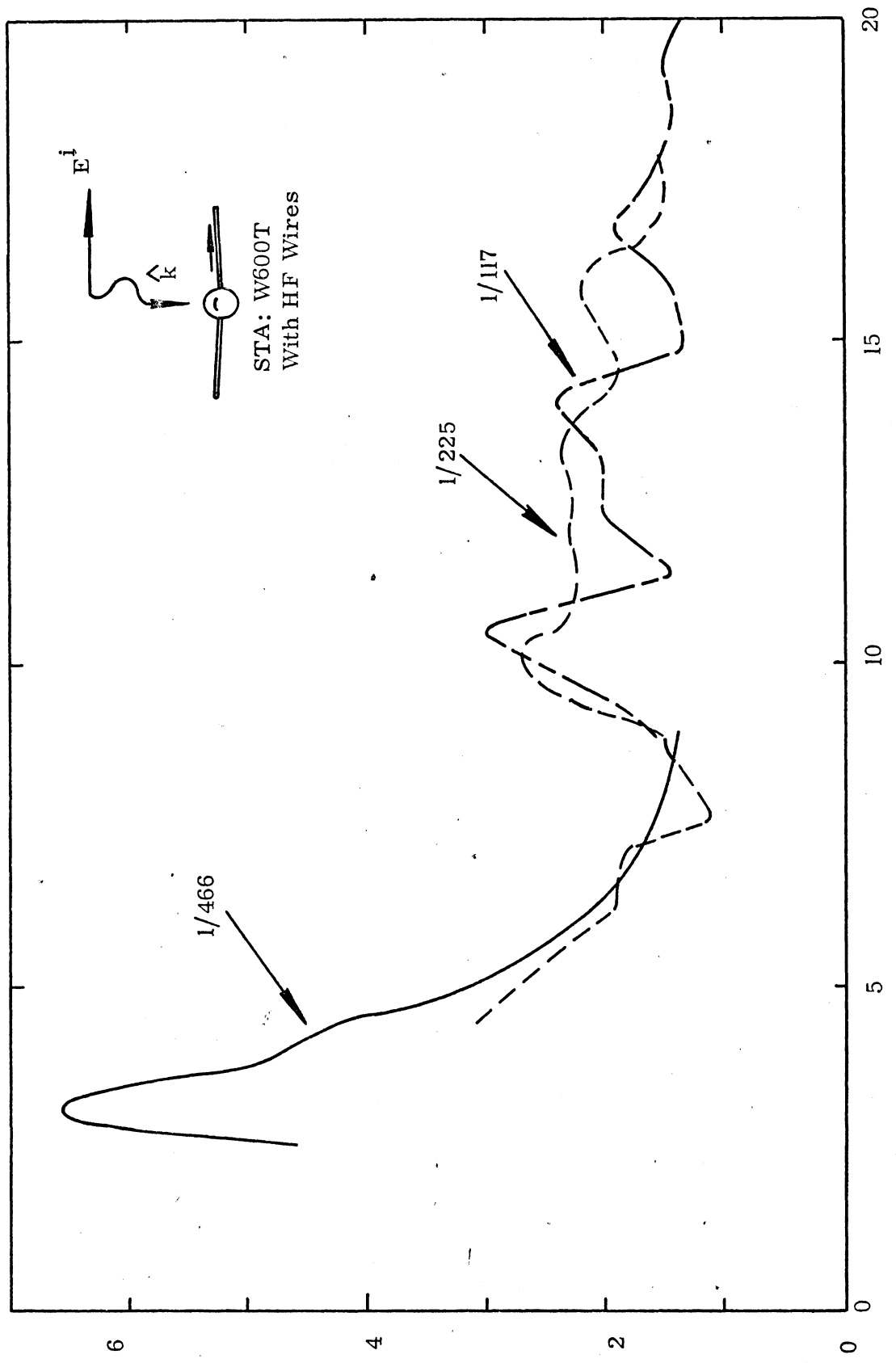

Figure 19a: Current Density at STA: W600T, With HF Wires, Anti-symmetric excitation

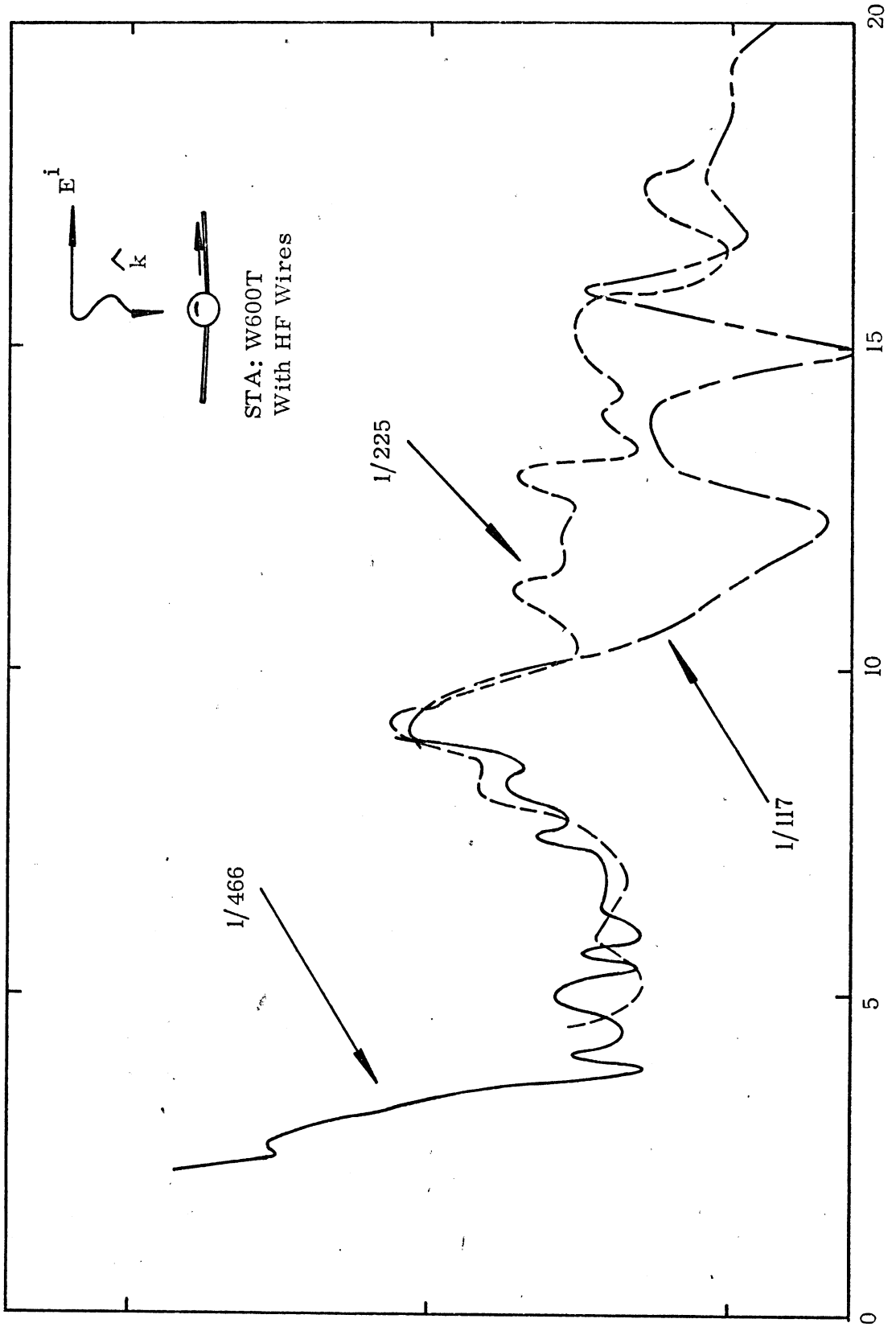

Figure 19b Current Phase At STA: W600T, With HF Wires, Anti-symmetric Excitation

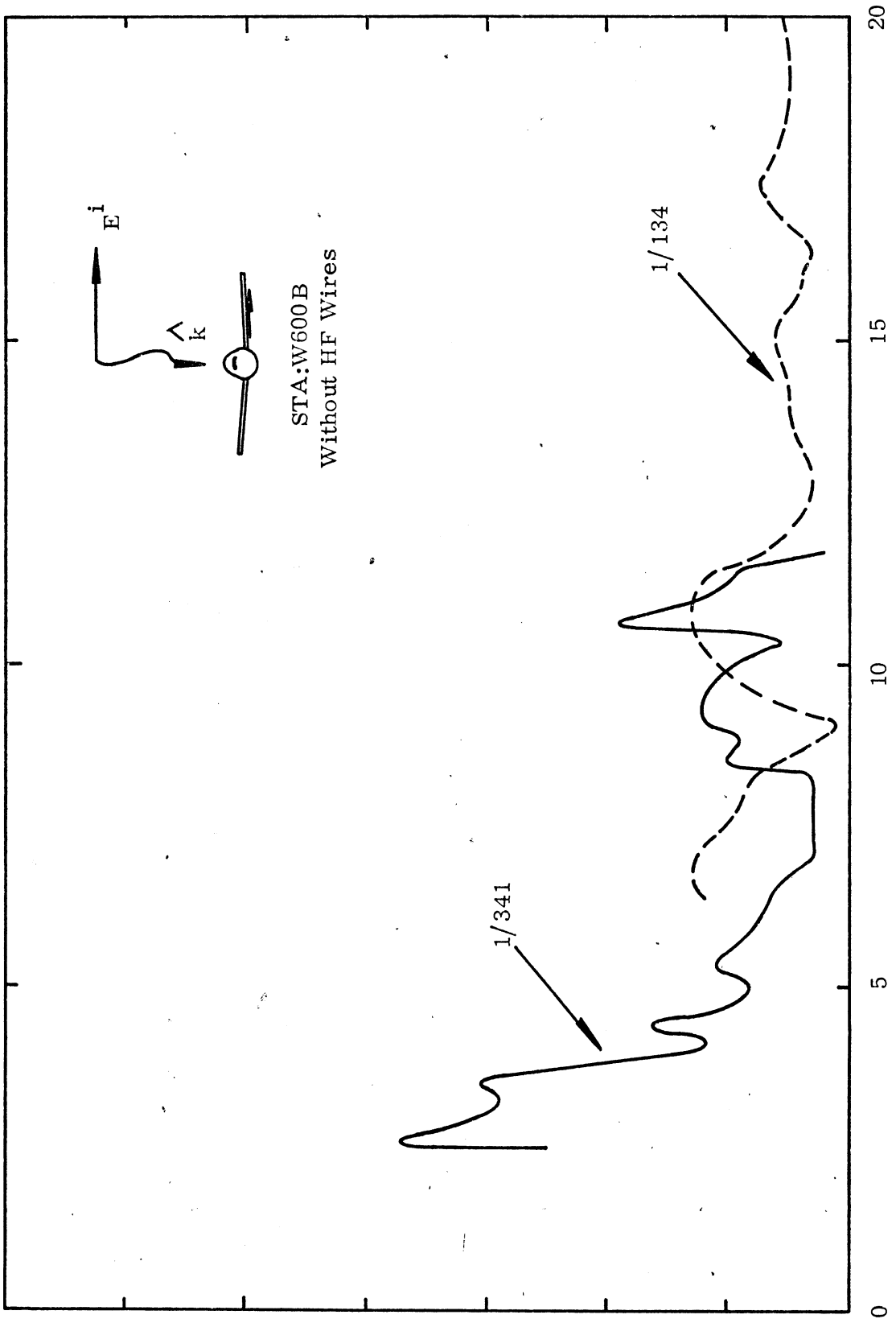

Figure 20: Current Density at STA:W600B, Anti-symmetric Excitation, Without HF Wires

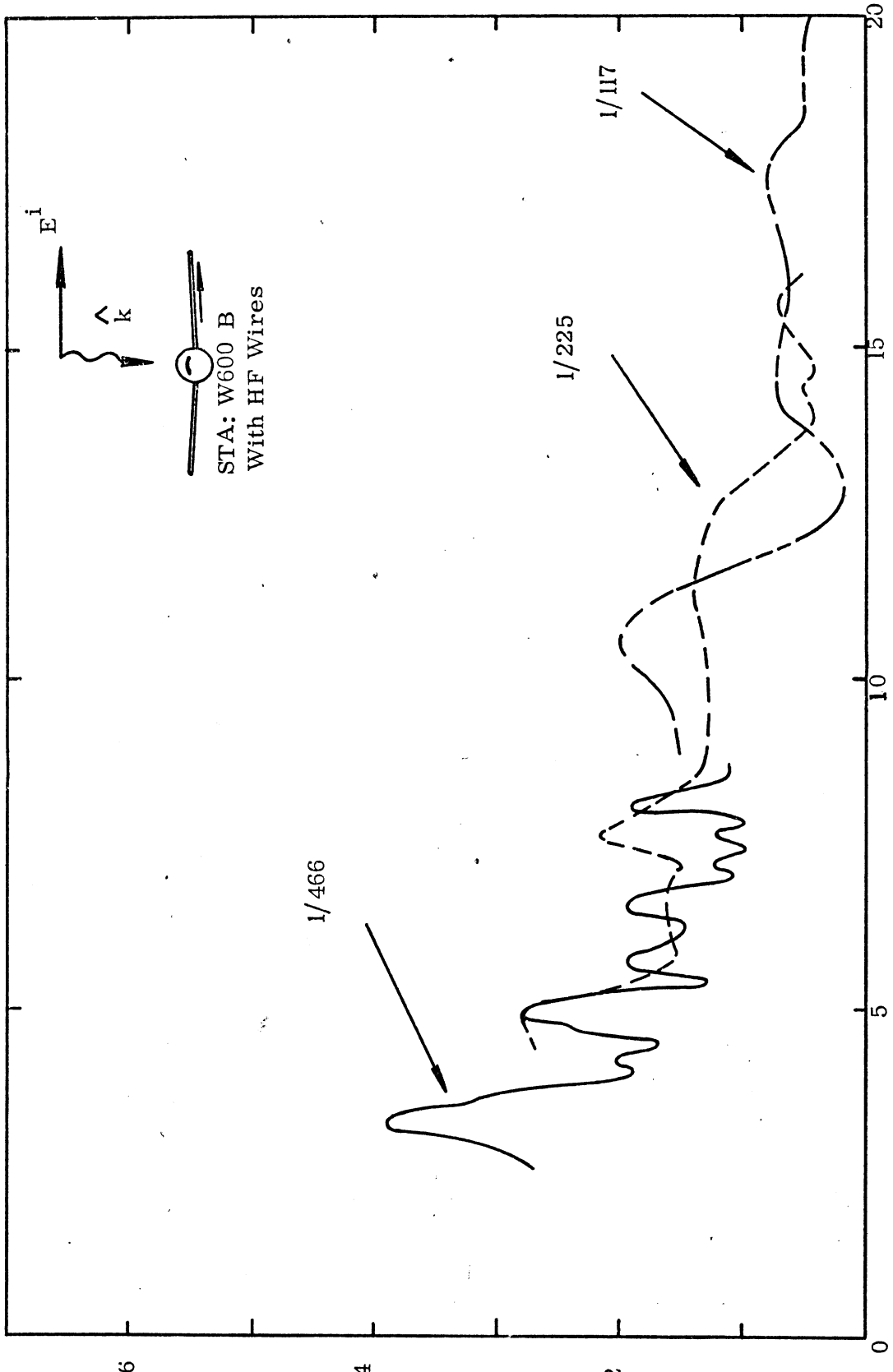

Figure 21: Current Density at STA: W600B, With HF Wires, Anti-symmetric Excitation

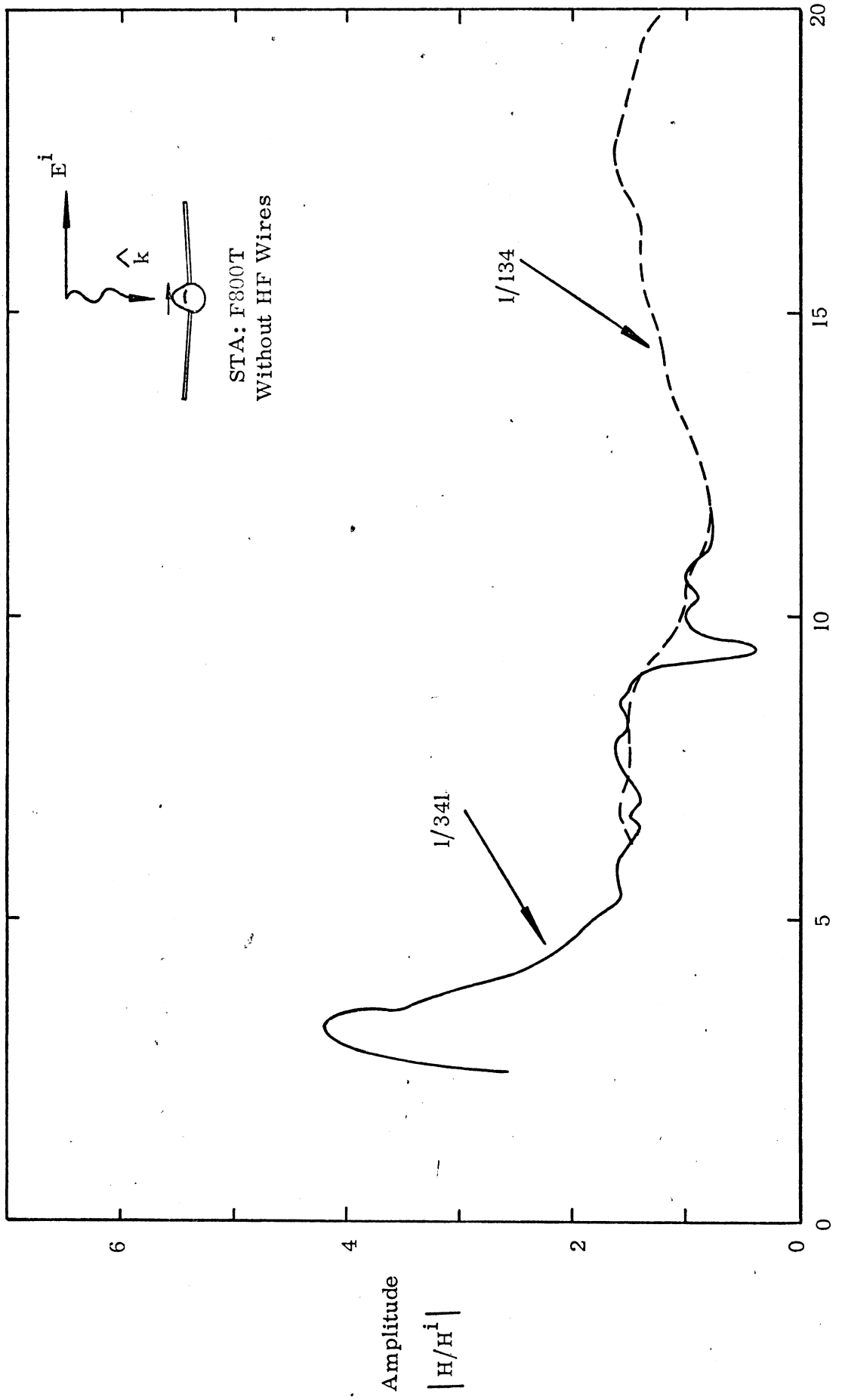

Figure 22a: Current Density at STA: F800T, Without HF Wires, Anti-symmetric Excitation

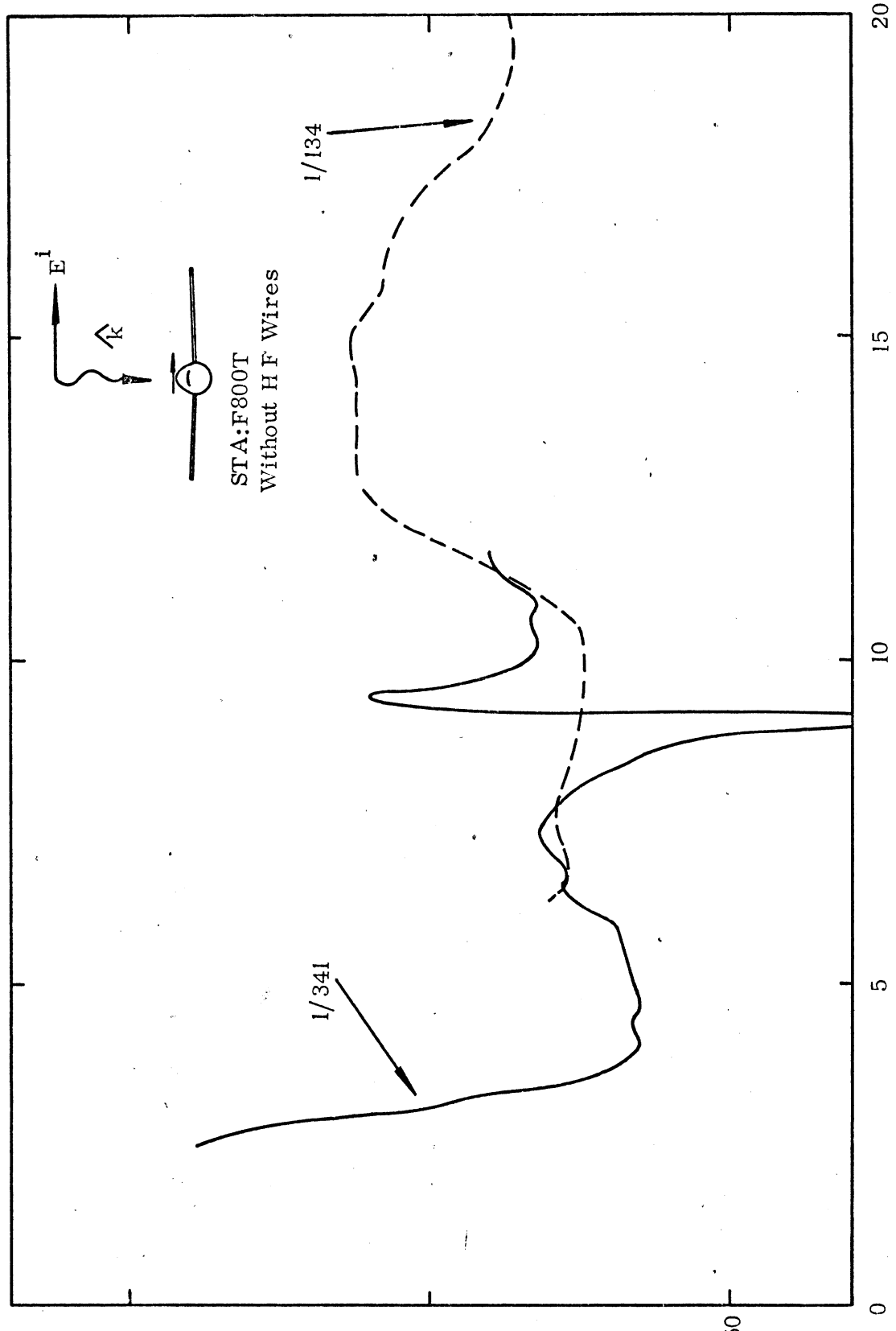

Figure 22b: Current Phase at STA: F800T, Without HF Wires, Anti-symmetric Excitation

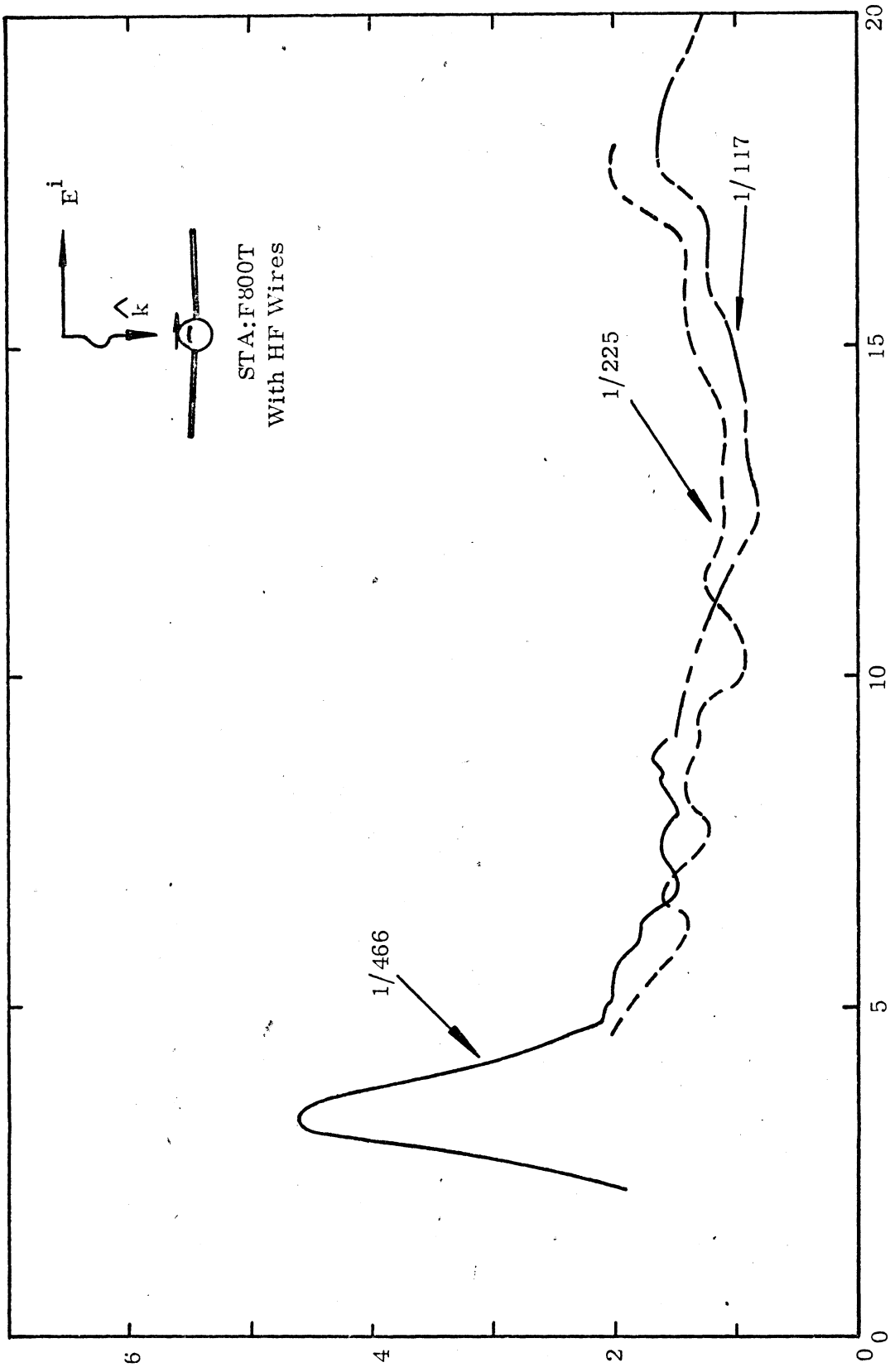

Figure 23a: Current Density at STA:F800T, Anti-symmetric Excitation, with HF Wires

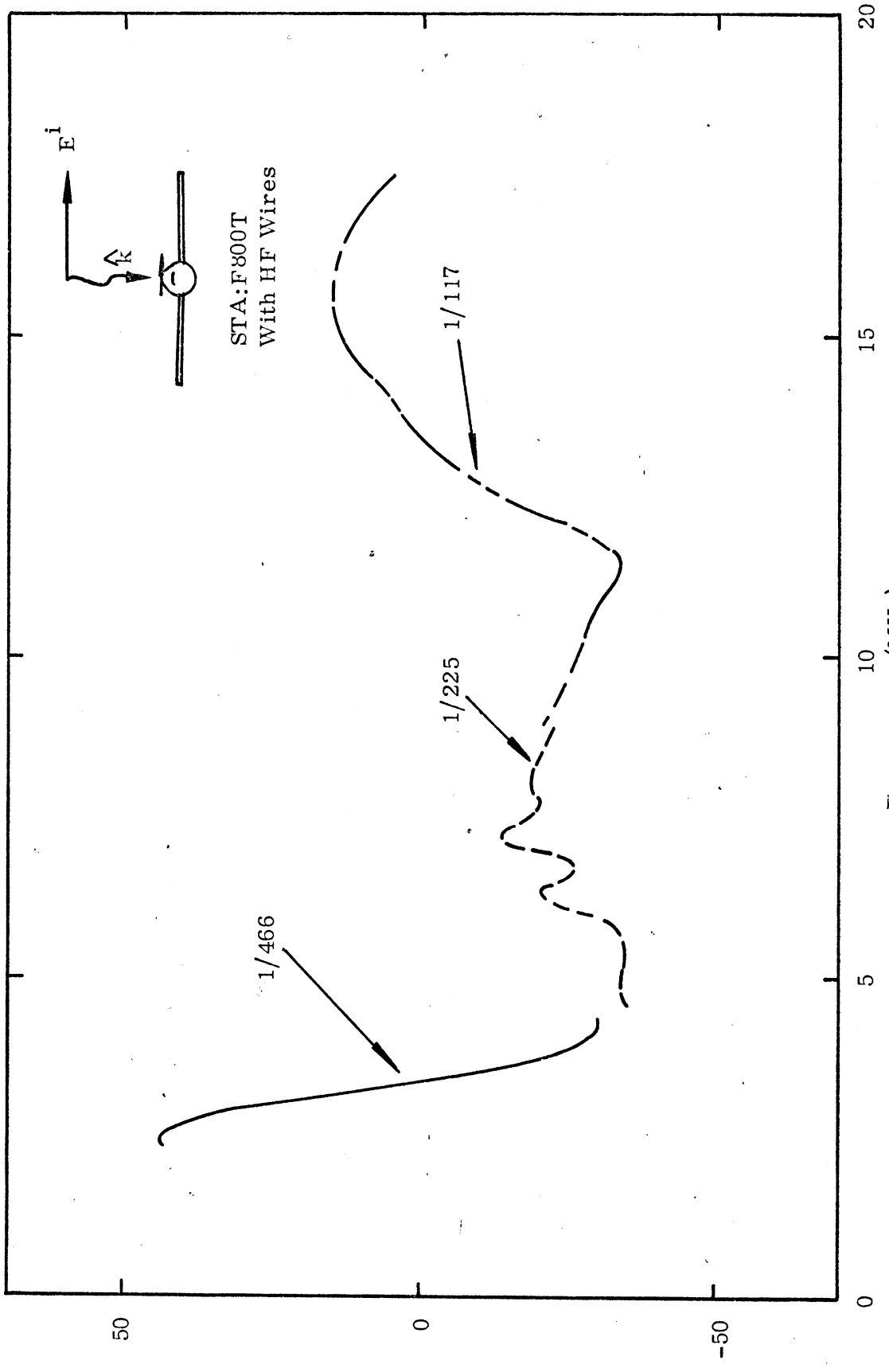

Figure 23b: Current Phase at STA:F800T, Anti-symmetric Excitation, with HF Wires

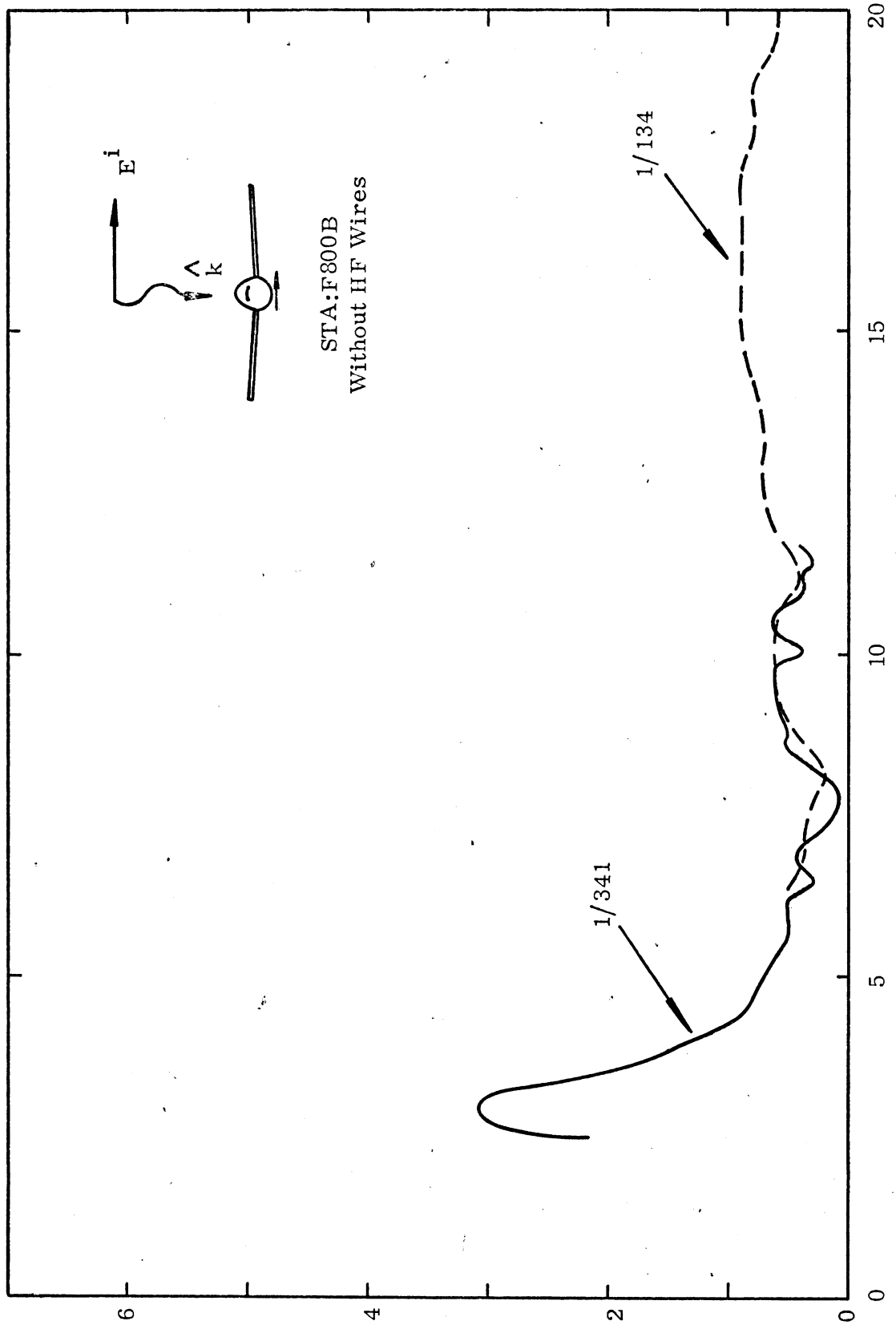

Figure 24: Current Density at STA:F800B, Anti-symmetric Excitation, Without HF Wires

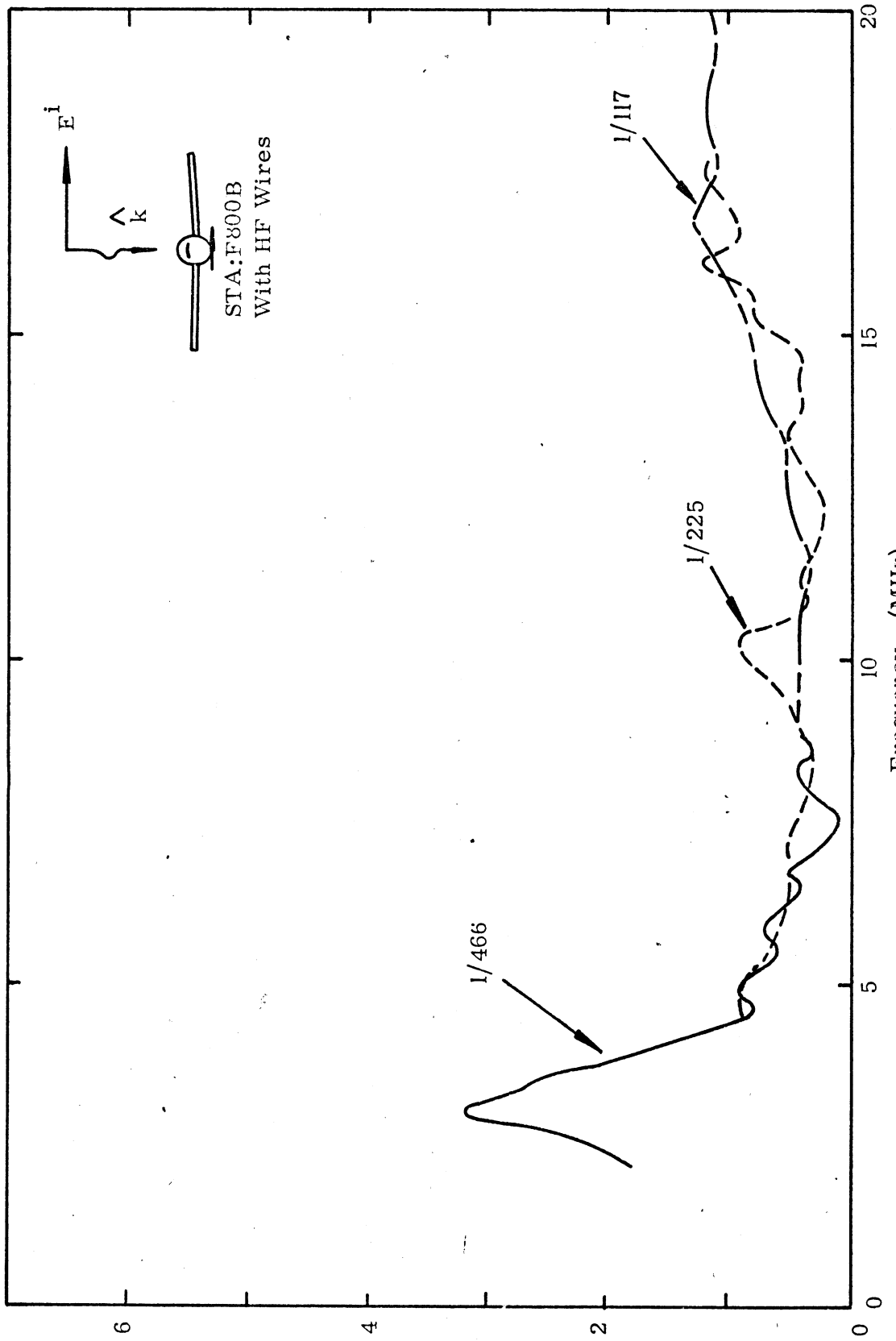

Figure 25: Current Density at STA:F800B, Anti-symmetric Excitation, with HF Wires

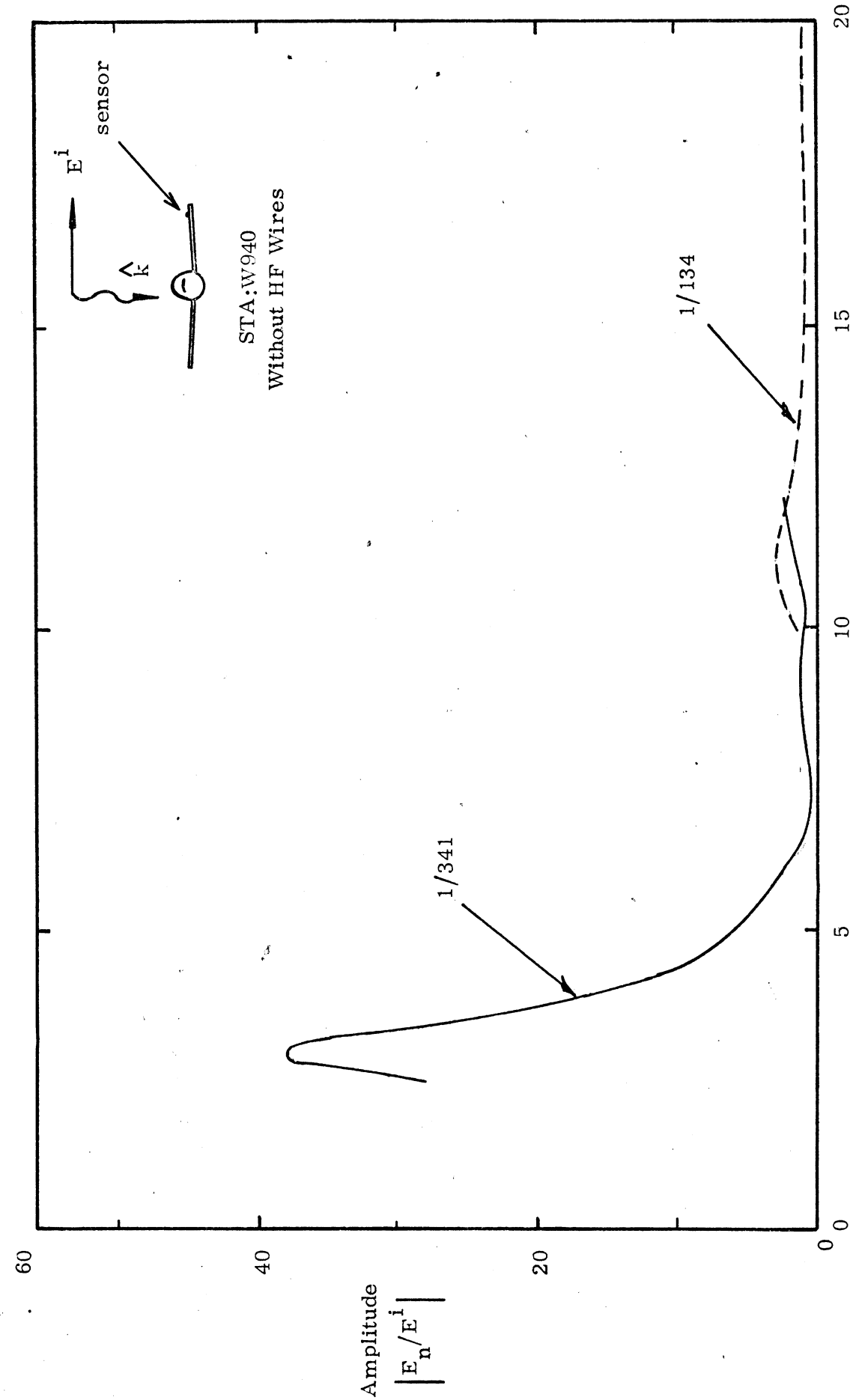

Figure 26: Charge Density at STA:W940, Anti-symmetric Excitation, without HF Wires

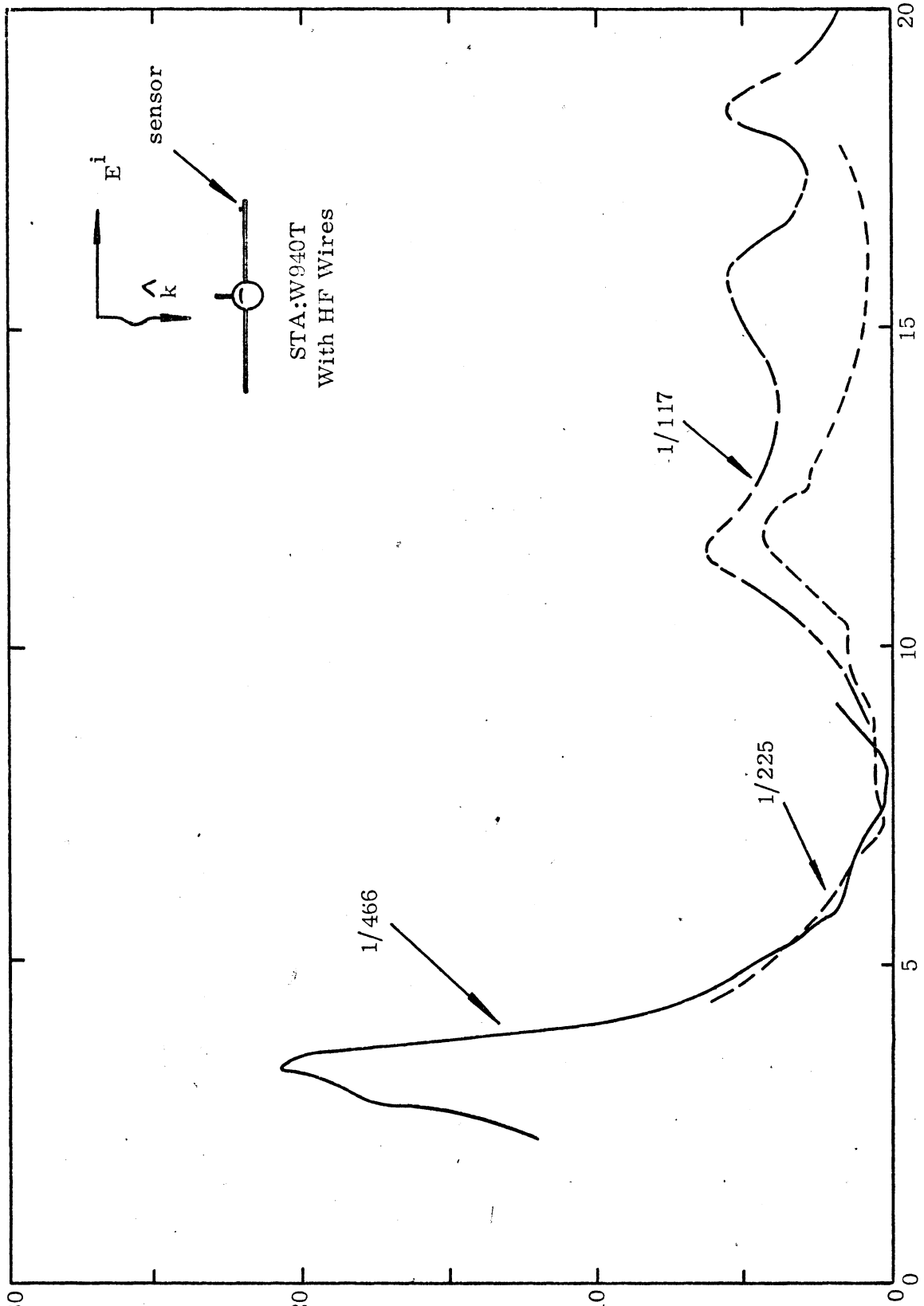

Figure 27: Charge Density at STA:W940T, Anti-symmetric Excitation, with HF Wires